AD-A158 445 TRANSPORT OF ANION IMPURITIES THROUGH OXIDES(U) ARIZONA 1/1
STATE UNIV TEMPE CENTER FOR SOLID STATE SCIENCE
J B WAGNER 02 JUL 85 ARO-18043.7-MS DAAG29-81-K-0109
UNCLASSIFIED F/G 7/4 NL

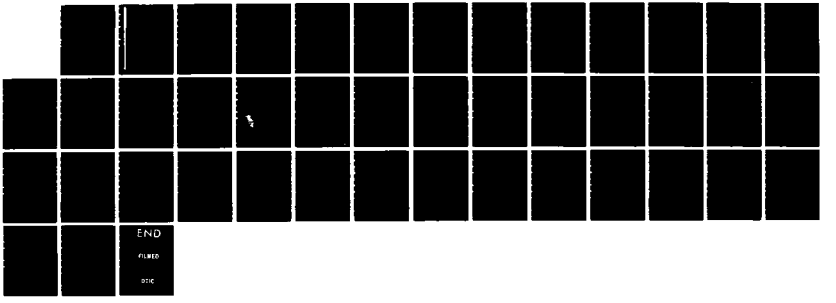

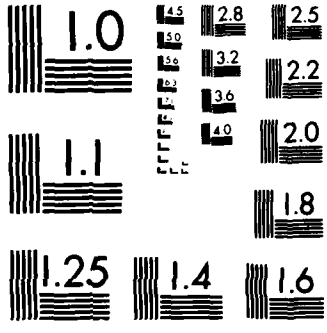

MICROCOPY RESOLUTION TEST CHART

ARO 18043.7-MS

(2)

TRANSPORT OF ANION IMPURITIES THROUGH OXIDES

FINAL REPORT FOR THE PERIOD
1 JULY 1981 THROUGH 30 JUNE 1985

BY

J. BRUCE WAGNER, JR.

JULY 2, 1985

TO

U.S. ARMY RESEARCH OFFICE

CONTRACT DAAG29-81-K-0109

CENTER FOR SOLID STATE SCIENCE
ARIZONA STATE UNIVERSITY
TEMPE, AZ 85287

APPROVED FOR PUBLIC RELEASE
DISTRIBUTION UNLIMITED

TRANSPORT OF ANION IMPURITIES THROUGH OXIDES

FINAL REPORT FOR THE PERIOD
1 JULY 1981 THROUGH 30 JUNE 1985

BY

J. BRUCE WAGNER, JR.

JULY 2, 1985

TO

U.S. ARMY RESEARCH OFFICE

CONTRACT DAAG29-81-K-0109

CENTER FOR SOLID STATE SCIENCE
ARIZONA STATE UNIVERSITY
TEMPE, AZ 85287

APPROVED FOR PUBLIC RELEASE
DISTRIBUTION UNLIMITED

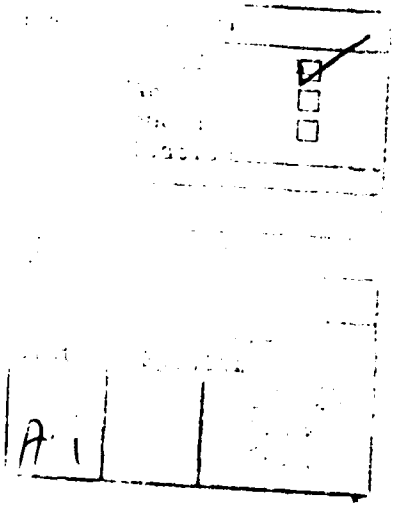

SECURITY CLASSIFICATION OF THIS PAGE *(When Data Entered)*

REPORT DOCUMENTATION PAGE		READ INSTRUCTIONS BEFORE COMPLETING FORM
1. REPORT NUMBER ARO 18043.7-MS	2. GOVT ACCESSION NO. AD-A158 445	3. RECIPIENT'S CATALOG NUMBER
4. TITLE *(and Subtitle)* TRANSPORT OF ANION IMPURITIES THROUGH OXIDES		5. TYPE OF REPORT & PERIOD COVERED FINAL: 7/1/81-6/30/85
		6. PERFORMING ORG. REPORT NUMBER
7. AUTHOR(s) J. BRUCE WAGNER, JR.		8. CONTRACT OR GRANT NUMBER(s) DAAG29-81-K-0109
9. PERFORMING ORGANIZATION NAME AND ADDRESS ARIZONA STATE UNIVERSITY CENTER FOR SOLID STATE SCIENCE TEMPE, AZ 85287		10. PROGRAM ELEMENT, PROJECT, TASK AREA & WORK UNIT NUMBERS
11. CONTROLLING OFFICE NAME AND ADDRESS U.S. ARMY RESEARCH OFFICE P.O BOX 12211 RESEARCH TRIANGLE PARK, NC 27709		12. REPORT DATE JULY 2, 1985 13. NUMBER OF PAGES 52
14. MONITORING AGENCY NAME & ADDRESS *(if different from Controlling Office)* DR. G. MAX IRVING ADMIN. CONTRACTING OFFICER OFFICE OF NAVAL RESEARCH RESIDENT REP. BANDOLIER HALL WEST - ROOM 204 UNIVERSITY OF NEW MEXICO ALBUQUERQUE, NM 87131		15. SECURITY CLASS. *(of this report)* 15a. DECLASSIFICATION/DOWNGRADING SCHEDULE

16. DISTRIBUTION STATEMENT (of this Report)

Approved for public release; distribution unlimited.

17. DISTRIBUTION STATEMENT *(of the abstract entered in Block 20, if different from Report)*

NA

18. SUPPLEMENTARY NOTES

The view, opinions, and/or findings contained in this report are those of the author(s) and should not be construed as an official Department of the Army position, policy, or decision, unless so designated by other documentation.

19. KEY WORDS *(Continue on reverse side if necessary and identify by block number)*

Electrical Conductivity, Galvanic Cells, Composites, Thermodynamics, Sulfides

20. ABSTRACT *(Continue on reverse side if necessary and identify by block number)*

This research was divided into four interrelated parts. It was an outgrowth of an investigation on the corrosion of nickel in SO_2+Ar and in SO_2+SO_3+Ar gas mixtures at 800°C which was supported under previous ARO grants [DAAG29-78-G-0032; DAAG29-78-G-0060]. From the earlier studies it became clear that the transport properties of the sulfide, the oxidation of the sulfide itself and the transport properties of the duplex scale were needed data. In addition, the thermodynamics of the sulfides were needed.

DD FORM 1 JAN 73 1473 EDITION OF 1 NOV 65 IS OBSOLETE
S/N 0102-014-6601

SECURITY CLASSIFICATION OF THIS PAGE *(When Data Entered)*

Accordingly the following research was performed:

1. Transport Properties of $Ni_{3\pm x}S_2$
   a) electrical conductivity
   b) chemical diffusivity
   c) radio tracer sulfur diffusion
2. Gibbs Free Energy of $Ni_{3\pm x}S_2$ and $Fe_{1-x}S$ by Galvanic Cells
3. Oxidation of $Ni_{3\pm x}S_2$ in oxygen at 700°C
4. Transport in NiO-Ni_3S_2 composites

In what follows, a brief summary of each research objective is presented followed by the publications and extended abstracts which contain the details.

FORWARD

In energy systems, the problems associated with high temperature corrosion especially in mixed oxidants, e.g. oxygen containing sulfur dioxide and sulfur trioxide have limited the use of many materials because of the formation of sulfide layers and/or inclusions in duplex corrosion product scales. These corrosion products yield extremely poor corrosion resistance. In the present research we have studied the transport properties, the thermodynamics and free energy of formation of $Ni_{3\pm x}S_2$ and transport in synthetic composite scales of $Ni_{3\pm x}S_2$ and NiO. We have also studied the oxidation of $Ni_{3\pm x}S_2$ as a function of sulfur concentration. The free energy of $Fe_{1-x}S$ was also determined.

Statement of the Problem

Many high temperature corrosion processes are determined by the transport of reactants through a duplex (two phase) scale. In the particular case of corrosion of nickel base alloys, corrosion in oxygen containing SO_2 and SO_3 results in the formation of a duplex scale consisting of nickel sulfide(s) and one or more oxides depending on the alloy composition, the temperature and gas composition. For high concentrations of nickel, the scales often consist of $Ni_{3\pm x}S_2$ as a separate layer, as islands embedded in the oxide or as channels or stringers through the oxide. The thermodynamic and the transport properties of $Ni_{3\pm x}S_2$ were not known. We undertook the present studies to contribute to an understanding of corrosion in mixed oxidants at elevated temperatures.

1. Transport Properties of $Ni_{3\pm x}S_2$.

The limits of the phase field of β-$Ni_{3\pm x}S_2$ were determined using H_2/H_2S gas mixtures and thermogravimetric analyses at 600° and 750° C. The existence of β_1, and β_2-$Ni_{3\pm x}S_2$ was confirmed. Thus a contribution to the phase diagram and to the thermodynamics of the Ni-S system was made. Utilizing a relaxation technique, the nickel sulfide was equilibrated with a given ratio of H_2/H_2S. This ratio was abruptly and isothermally changed to another ratio and the kinetics of re-equilibration with the new value of the H_2/H_2S ratio was carried out using TGA. Therefrom the chemical diffusion coefficient, $\tilde{D}$, was calculated. It was found that $\tilde{D}$ varied with stoichiometry and exhibited a maximum at the stoichiometric composition, Ni_3S_2. The diffusivities were in reasonable agreement with the only other literature values by A. Stoklosa and J. Stringer [Oxidation of Metals 11, 277 (1977)].

The electrical conductivity of stoichiometric Ni_3S_2 was determined between 50° and 750° C. The resistance increased with temperature indicative of metallic behavior. In addition, the electrical conductivity was measured as a function of composition at 650°C. The conductivity increased with increasing mole fraction of sulfur. More structural data are needed in order to put forward a defect model or models consistent with these data.

The transport rate in $Ni_{3\pm x}S_2$ was determined to be extremely rapid, with $\tilde{D}$ of the order of 10^{-5} to 10^{-6} cm^2/sec at 700° and 650°C, respectively. Radio-tracer sulfur-35 measurements were made in $Ni_{3\pm x}S_2$ containing 40 and 42 at % S. The diffusivity of sulfur

at 695° and at 775° C was about 10^{-10} and 10^{-8} cm^2/sec, respectively. This indicates that the diffusivity of nickel is responsible for the rapid transport in $Ni_{3\pm x}S_2$.

2. Free Energy of $Ni_{3\pm x}S_2$ and $Fe_{1-x}S$.

An indirect method utilizing a galvanic cell was used to obtain the free energy of formation of $Ni_{3\pm x}S_2$. The cell was of the following configuration:

Pt, Air|YSZ|NiO, $Ni_{3\pm x}S_2$, SO_2 (1 atm), Pt (A)

Because the free energies of NiO and SO_2 are known, the free energy of $Ni_{3\pm x}S_2$ can be calculated from the open circuit EMF of cell (A). The results were

$\Delta G^\circ(Ni_3S_2,s) = -74,740+31.007T$ in cal/mole

and

$\Delta G^\circ(Ni_3S_2,l) = -60,420+17.855T$ in cal/mole

and the enthalpy of fusion for Ni_3S_2 was 14,320 cal/mole at 1089K.

As complementary information, the free energy of $Fe_{1-x}S$ was also determined using a similar galvanic cell,

Pt,Air|YSZ|$Fe_{1-x}S$, Fe_3O_4, SO_2 (1 atm), Pt (B)

whence

$\Delta G^\circ(Fe_{1-x}S) = -40,733+15.7712T-x(-34,403+14.0525T)$ in cal/mole.

(3) Oxidation of $Ni_{3\pm x}S_2$ as a function of stoichiometry at 700°C.

When nickel or a nickel alloy is exposed to oxygen containing SO_2 and SO_3 at elevated temperatures, a duplex scale consisting of NiO containing $Ni_{3\pm x}S_2$ forms. The corrosion process continues by not only the transport of ion and electrons (primarily nickel and electron holes) but also the oxidation of the sulfides. While this oxidation is most often reported when the sulfide is extruded

through the scale to the scale-gas interface, it can certainly also proceed within the scale. Moreover, the stoichiometry of the $Ni_{3\pm x}S_2$ is very likely dependent on its position relative to the metal-scale and the scale-gas interfaces. Accordingly, we undertook a study of the oxidation of $Ni_{3\pm x}S_2$ as a function of x. Briefly, at low sulfur activities, the reaction is slow and the rate determining step is transport through a relatively compact and coherent NiO layer (weight gain of sample). On the other hand, at high sulfur activities, a gaseous product (SO_2 and/or SO_3) is formed which ruptures the NiO film and results in very rapid corrosion (weight loss of sample). These results are important to the overall understanding of the kinetics and mechanism of corrosion.

(4) Transport in Two Phase Ni_3S_2-NiO Synthetic Corrosion Product Scales.

When small, insoluble metallic particles are dispersed in a semiconductor, the transport properties of the composite can be radically altered. In the present case, $Ni_{3\pm x}S_2$, was shown to be a metallic conductor. NiO is a p-type semiconductor. Around each $Ni_{3\pm x}S_2$ particle there is a space change layer of electrons according to a theory developed by C. Wagner [J. Phys. Chem. Solids 33, 1051 (1972)]. Accordingly, as more Ni_3S_2 particles are added to NiO, the electrical conductivity decreases (by 10^3), goes through a minimum and then increases. Seebeck coefficient measurements indicate that the conductivity at low concentrations of Ni_3S_2 is p-type but composites containing the higher concentrations are n-type! This can be explained by the fact that the

electrons in the space charge layer annihilate the electron holes in the NiO. Thus the electrical conductivity decreases with additions of $Ni_{3\pm x}S_2$, goes through a minimum (corresponding to a p to n transition) and then increases by n-type conduction. This phenomenon in itself is a remarkable guide to heterogeneous doping and it is the first time such an effect has been reported.

From the point of view of corrosion, the defects in NiO are described by

$$1/2\ O_2(gas) = O_0 + V''_{Ni} + 2h^{\bullet}$$

whence

$$K = [V''_{Ni}][h^{\bullet}]^2 / P_{O_2}{}^{1/2}$$

Thus for an isothermal corrosion process under constant oxygen pressure, adding electrons (from the insoluble Ni_3S_2) will decrease the concentration of electron holes as is observed from conductivity measurements. Consequently there should be a corresponding increase in cation vacancy concentration. While this is an equilibrium arguement, the trend is clear for a kinetic situation and an additional possibility for the rapid corrosion of nickel in O_2-SO_2 gas mixtures has been advanced.

List of All Publications and Technical Reports

1. G.M. Mehrotra and J.B. Wagner, Jr., "On the Thermodynamic Properties of $Fe_{1-x}S$", extended abstract submitted to The Electrochemical Society for presentation at Las Vegas meeting, October 13-18, 1985.

2. G.M. Mehrotra, V.B. Tare and J.B. Wagner, Jr., "The Standard Free Energy of Formation of $Ni_{3+x}S_2$", J. Electrochem. Soc. 132, 247-250 (1985); also published in Proc. Vol. 83-7, Symposium on High Temperature Material Chemistry II, Ed. by Z.A. Munir and D. Cubbicciotti, The Electrochemical Society (1983).

3. G.M. Mehrotra, V.B. Tare and J.B. Wagner, Jr., "Oxidation of Nickel Sulfides in Oxygen at 700 C", J. Electrochem. Soc. 132, 244-247 (1985); also published in Proc. Vol. 83-7, Symposium on High Temperature Material Chemistry II, Ed. by Z.A. Munir and D. Cubbicciotti, The Electrochemical Society (1983).

4. V.B. Tare and J.B. Wagner, Jr., "Electrical Conduction in Two-Phase Nickel Oxide-Nickel Sulfide Mixtures", J. Appl. Phys., 54(1), 252-257 (1983).

5. H. Yagi and J.B. Wagner, Jr., "Chemical Diffusion and Electrical Conductivity of $Ni_{3+x}S_2$", Oxidation of Metals 18 nos. 1/2, 41-54 (1982).

6. G.M. Mehrotra and J.B. Wagner, Jr., "Diffusion of Sulfur in $Ni_{3+x}S_2$", Extended Abstract No. 11, The Electrochemical Society, Cincinnati, Ohio, May 6-11, 1984.

Thesis Awarded

H. Yagi, "Corrosion of Nickel at 800° C in SO_2+Ar and SO_2+O_2+Ar Atmospheres", PhD Thesis, Arizona State University, May 1982.

Submitted to the Electrochemical Society Meeting Scheduled for Las Vegas, October 13-18, 1983.

ON THE THERMODYNAMIC PROPERTIES OF $Fe_{1-x}S$

G. M. Mehrotra and J. B. Wagner, Jr.

Center for Solid State Science
Arizona State University
Tempe, Arizona 85287 USA

Ferrous sulfide is known to have a wide range of non-stoichiometry. The thermodynamics of FeS have been studied by several investigators. Ramanarayanan and Worrell [1] and Oishi, et al. [2] have determined the Gibbs energy of formation of stoichiometric FeS using galvanic cells employing CaF_2 as solid electrolyte. There are, however, no data for non-stoichiometric $Fe_{1-x}S$. In the present work, thermodynamic properties of $Fe_{1-x}S$ have been determined, in the temperature range 600° to 1000°C, using solid state galvanic cells with yttria stabilized zirconia as the solid electrolyte.

Galvanic cells of the configuration

$$Pt, air|YSZ|Fe_{1-x}S, Fe_3O_4, SO_2\ (1\ atm), Pt \qquad (A)$$

have been used in the present investagtion. Cells of similar configuration have been successfully used earilier by the authors [3] for the thermodynamic studies on $Ni_{3+x}S_2$ and by Elliott, et al. [4] for the study of PtS, TaS_2, NbS_2, MoS_2 and MnS_2. One-end closed tubes of yttria-stabilized zirconia served as the solid electrolyte. The chemicals used in our studies (FeS and Fe_3O_4) were puratronic grade purchased from Johnson-Matthey. SO_2 was passed over Drierite and P_2O_5. Since, under our experimental conditions, the pressure of SO_3 in equilibrium with SO_2 and O_2 is negligible, (5.06×10^{-8} to 1.11×10^{-6} atm), no correction for SO_3 has been applied and the pressure of SO_2 has been taken to be 1 atm. The open circuit emf of the cells was measured in the temperature range 550° to 1000 °C using a Keithly high-impedance multimeter. The temperature of the cell was measured using a Pt - 10% Rh/Pt thermocouple.

Figure 1 shows the results of our measurements from five different cells. In one of the cells, FeS_2 was substituted for FeS. It can be seen that the values of emf are identical, within experimental error limits, in the temperature range of our study. This suggests that, at any given temperatrue, the composition of $Fe_{1-x}S$ in equilibrium with Fe_3O_4 and SO_2 (1 atm) is fixed. This observation is similar to the one we made in our thermodynamic study of $Ni_{3+x}S_2$. The $\frac{S}{Fe}$ ratio in $Fe_{1-x}S$ in equilibrium with Fe_3O_4 and SO_2 (1 atm) is being determined.

In the temperature range of our investigation, iron undergoes two transformations, viz α - β at 770°C and β - γ at 912°C. The relationship between the experimentally determined values of emf and temperature can, however, be satisfactorily described by the linear equation

$$E = 868.5 - 0.2033\ T$$

where E is the emf of cell (A) in mV and T is temperature in Kelvin.

The virtual cell reaction for the cell (A) is

$$3\ Fe_{1-x}S + (5 - 2x)O_2 = (1 - x)Fe_3O_4 + 3\ SO_2$$

Therefore,

$$\Delta G_{cell} = 3\Delta G^{\circ}_{SO_2} + (1 - x)\Delta G^{\circ}_{Fe_3O_4} - 3\Delta G^{\circ}_{Fe_{1-x}S} - (5 - 2x)\ RT\ln P_{O_2}\ (air)$$

Substituting for ΔG_{cell}, we obtain

$$3\Delta G^{\circ}_{Fe_{1-x}S} = 3\Delta G^{\circ}_{SO_2} + (1 - x)\Delta G^{\circ}_{Fe_3O_4} + 4F(5 - 2x)(E + 0.03362\ T)$$

where F is Faraday's constant.

Using the reported data for the Gibbs energy of formation of Fe_3O_4 and SO_2, one obtains

$$\Delta G^{\circ}_{Fe_{1-x}S} = -40{,}733 + 15.7712\ T - x(-34{,}403 + 14.0525\ T)\ \text{in cal/mole} \qquad (B)$$

In Figure 2 are plotted the values of ΔG°_{FeS} and $\Delta G^{\circ}_{Fe_{0.9}S}$ as calculated using eq. (B). It can be seen that the values of ΔG°_{FeS} obtained in the present work are lower by about 2kcal/mole compared to the values obtained by earlier investigators [1,2] from measurements using galvanic cells with a CaF_2 electrolyte. It is interesting to note that the values of ΔG°_{FeS} reported by Ramanarayanan and Worrell [1] and by Oishi, et al. [2] are in very good agreement with the values of $\Delta G^{\circ}_{Fe_{0.9}S}$ as obtain from our eq. (B). The literature values of ΔG°_{FeS} which are closest to ours are those reported by Turkdogan [5]. As the emf values obtained in our studies were very reproducible during heating as well as cooling, and as the attainment of equilibrium was rapid, the values obtained in this work are considered reliable.

ACKNOWLEDGEMENT

This research was sponsored by the Army Research Office under contract DAAG29-81-K-0109 and a grant from the Center for Solid State Science.

REFERENCES

[1]. T. A. Ramanarayanan and W. Worrell, J. Electrochem. Soc., 127, 1717 (1980).
[2]. T. Oishi, T. Fujimura, K. Ogura and J. Moriyama, J. Japan Institute of Metals, 40, 969 (1976).
[3]. G. M. Mehrotra, V. B. Tare and J. B. Wagner, Jr., J. Electrochem. Soc., 132, 247 (1985).
[4]. J. F. Elliott and H. R. Larson, Trans. Met. Soc. AIME, 239, 1713 (1967).
[5]. E. T. Turkdogan, Physical Chemistry of High Temperature Technology, Academic Press, New York, Chapter 1 (1980).
[6]. O. Kubaschewski, E. Ll. Evans and C. B. Alcock, Metallurgical Thermodynamics, Pergamon Press, New York (1967).

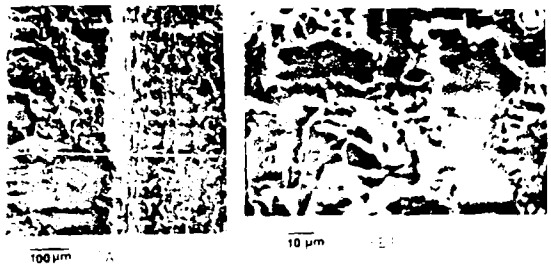

Fig. 4 SEM picture of nickel sulfide containing 39 a/o S. (A): Cross section of the oxidized specimen. (B): Surface of the oxidized specimen.

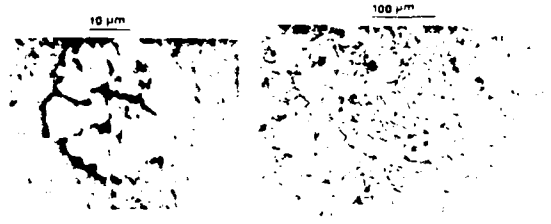

Fig. 5 SEM picture of nickel sulfide containing 38 a/o S. (A): Unoxidized Ni_xS particle in the interior of the specimen. (B): Line scan across the above specimen. (C): Surface of the oxidized specimen.

$$Ni_xS_y + \left(\frac{7+x}{2}\right)O_2 = (3+x)NiO + 2SO_2 \qquad [2]$$

$$Ni_xS_y + \left(\frac{9+x}{2}\right)O_2 = (3+x)NiO + 2SO \qquad [3]$$

Reaction [1] is characterized by the increase in weight of the sample due to oxidation without evolution of SO_2, whereas reactions [2] and [3] are associated with the decrease in weight because of evolution of SO_2 and/or SO as one of the reaction products. The initial weight increase observed during oxidation of Ni_xS_y is thus suggested to be due to the formation of NiO and simultaneous change in the stoichiometry of Ni_xS_y, in accordance with reaction [1]. This is followed by reaction [2] and/or [3], resulting in subsequent weight loss.

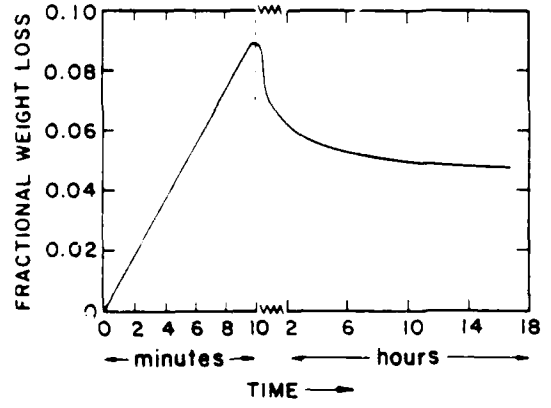

Fig. 6 Oxidation of NiS in oxygen at 700 C

In the present studies, negligibly small increase in weight during the initial stages of oxidation of nickel sulfide containing 42 a/o sulfur indicates that this is probably close to the limiting composition which favors the formation of NiO directly by reaction [2] and/or [3]. Any composition of nickel sulfide which contains nickel in excess of this limiting composition would result in a weight gain owing to the oxidation of excess nickel to NiO. The fractional weight increase calculated assuming that all the excess nickel oxidizes to form NiO is shown in Table I along with experimentally observed fractional weight increase. The agreement between the calculated and experimentally observed values, except for the starting composition of 39 a/o sulfur, is extremely good.

It is interesting to note that similar results were obtained by Asaki *et al.*, who studied the oxidation of dense pellets of FeS (3) at 750°-850°C and $p_{O_2} \sim 0.01$-0.2 atm, and of nickel sulfide (X_s = 0.4-0.44) (4) at 650°-750°C and $p_{O_2} \sim 0.2$ atm. They analyzed the exit gases formed during oxidation by infrared gas analysis and found that during oxidation of stoichiometric FeS, a very small amount of SO_2 was evolved in the initial 5s, and then it stopped for several hours afterward. The initial weight increase was explained by them to be due to the formation of Fe_3O_4 with the simultaneous change in the stoichiometry of FeS. In the case of oxidation of nickel sulfide, their results show that there is a weight increase in the initial stages of oxidation and that the progress of oxidation is dependent on the composition of nickel sulfide and temperature of oxidation. They found that, in the oxidation runs in which an increase in weight occurred, a very small amount of SO_2 was evolved during the initial 30s, and the evolution was even less during the subsequent period of weight increase. This shows that during the initial stages of oxidation with a weight increase, the rate of oxidation due to reaction [2] and/or [3] is negligible. No increase in the weight of the sample containing 44 a/o sulfur was observed by them during its oxidation at 700°C. The results of Asaki *et al.* are thus qualitatively in agreement with our results.

During the initial stages, the rate at which nickel oxide is formed is expected to be higher on compositions containing higher concentrations of nickel because of the larger concentration gradients. The subsequent reaction rate will, however, depend upon the morphology of the nickel oxide formed. It is interesting to note that, except for the composition containing 39 a/o S, the rate of weight loss after the initial weight gain is approximately the same. This is consistent with the view that, irrespective of the starting composition, the compositions at the start of reaction [2] and/or [3] above are approximately the same.

Almost complete protection offered by the formation of NiO on composition containing 39 a/o S may be attributed to the slow formation and hence a compact layer of NiO. In the case of nickel sulfide containing 38 a/o S, the rate of formation of NiO is relatively high and hence the resultant NiO layer is full of cracks as observed experimentally. However, the large number of cracks observed in NiO formed on compositions containing 40, 41.4, and 42 a/o S are possibly due to the simultaneous occurrence of reactions [1], [2], and/or [3] above, leading to the formation of SO

Table I Calculated and experimentally observed fractional weight increase during the initial stages of oxidation of various Ni_xS_y compositions

Initial a/o S in Ni_xS_y	Fractional weight increase calculated	Fractional weight increase experimental
42	0.000	0.000
41.4	0.007	0.005
40	0.015	0.015
39	0.023	0.010
38	0.031	0.030

at 700° ± 5°C. Prior to the beginning of oxidation, the $Ni_{1-y}S_2$ pellets were annealed at 700°C for at least 1h in a flowing stream of argon (oxygen content ~20 ppm) for homogenization. A small weight change (fractional weight change ~0.0005-0.003) was observed during this period. The kinetics of oxidation were followed by a 1000 Cahn electrobalance thermogravimetric setup. A chart recorder, connected to the electrobalance, continuously recorded the weight changes. These were replotted as the fractional weight changes calculated from the observed changes in weight and the initial weight of the sample. The weight changes observed during the annealing period were included in calculations. The time at which the argon gas flow was terminated and oxygen was started was taken as the starting time (t = 0).

Results

Figure 1 shows typical results from oxidation runs on $Ni_{1-y}S_2$ of five compositions. All the compositions showed an initial increase in weight, followed by a decrease in weight.

For compositions containing 41.4 and 42 a/o S, the initial increase was extremely small. For the 40.0 a/o S composition, the weight increased slowly for almost 6h, followed by a slow continuous decrease. The sample with 39 a/o S increased in weight within first hour after which the weight remained constant for several hours (~24h). The samples with 38 a/o S showed an initial sharp increase in weight within the first half-hour, followed by an almost linear decrease in weight. Significant initial increase in weight is thus observed for compositions containing 38, 39, and 40 a/o sulfur. The rate of increase, however, decreased with increasing sulfur percentage. The rate of oxidation for composition containing 39 a/o S became negligibly small after 1h.

X-ray powder diffraction patterns of samples after the oxidation runs indicated the presence of NiO and Ni_3S_2 phases only. The pellets were also examined under SEM and analyzed by EDAX for morphological details and phase identification.

Figure 2(A) shows the surface of an oxidized sample of nickel sulfide containing 42 a/o S. The surface appears to be very nonuniform. A line scan for Ni and S across the surface of the sample shows the presence of discontinuous layer of NiO along with unoxidized or partially oxidized porous nickel sulfide. The cross-sectional view of an almost completely oxidized sample is shown in Fig. 2(B). A line scan across this sample shows a sudden drop

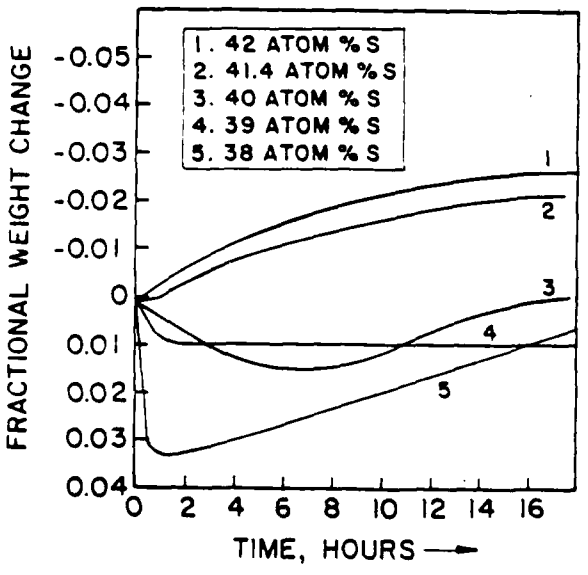

Fig. 1. Oxidation of Ni_3S_2 in oxygen at 700°C for various compositions.

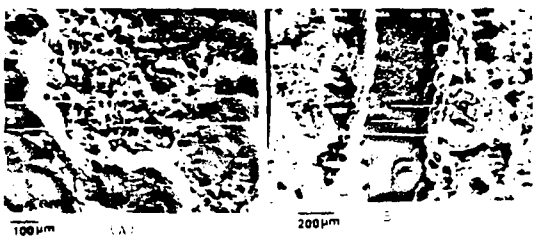

Fig. 2. SEM picture of nickel sulfide containing 42 a/o S. (A): Oxidized surface. (B): Cross section of the oxidized specimen.

in nickel concentration and absence of sulfur throughout the specimen, suggesting the presence of a cavity almost at the center of the pellet.

Figure 3(A) shows the cross section of an oxidized specimen containing 40 a/o S. A line scan for Ni and S across this is shown in Fig. 3(B). Two distinct regions identified as NiO and Ni_3S_2 are clearly seen in Fig. 3(A). The presence of occasional cracks in the NiO layer formed during oxidation is seen in Fig. 3(C).

Two distinct regions with nickel oxide at the surface and Ni_3S_2 underneath are also clearly identifiable in the cross-sectional view of the oxidized sample containing 39 a/o S [Fig. 4(A)]. The oxidized surface shown in Fig. 4(B) appears to be uniform and free from cracks.

A large number of cracks are found in the oxidized surface of samples with 38 a/o S [Fig. 5(C)]. Highly oxidized samples show the presence of isolated particles [Fig. 5(A)] identified by the line scan of nickel and sulfur [Fig. 5(B)] as nickel sulfide surrounded by nickel oxide.

Figure 6 shows the change in weight of NiS as a function of time during its oxidation in pure oxygen at 700°C. There is a very rapid, almost linear decrease in weight for the first 10 min, after which the weight slowly increases at a rate which decreases rapidly with time. The x-ray examination of the samples oxidized for 18h showed the presence of Ni_3S_2 and NiO phases only. The composition of Ni_3S_2 formed was not determined.

Discussion

The reaction of $Ni_{1-y}S_2$ with oxygen can be represented by the following equations

$$Ni_{1-y}S_2 + \frac{y-x}{2}O_2 = Ni_{1-x}S_2 + (y-x)NiO \quad 0 \leq x < y \qquad [1]$$

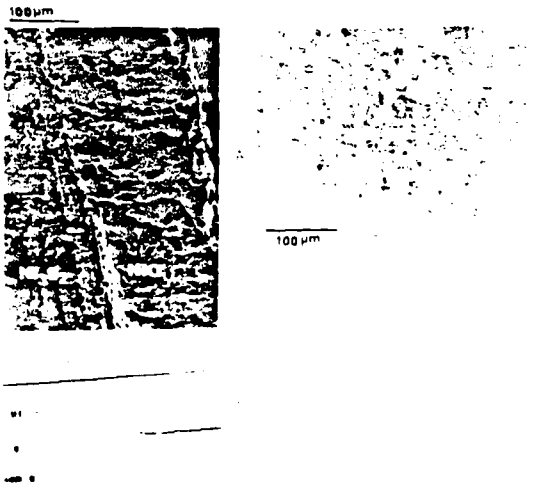

Fig. 3. SEM picture of nickel sulfide containing 40 a/o S. (A) Cross section of an oxidized specimen. (B) Line scan across the specimen. (C) Surface of an oxidized specimen.

Reprinted from JOURNAL OF THE ELECTROCHEMICAL SOCIETY
Vol. 132, No. 1, January 1985
Printed in U.S.A.

Oxidation of Nickel Sulfides in Oxygen at 700°C

G. M. Mehrotra,* V. B. Tare, and J. B. Wagner, Jr.*

Center for Solid State Science, and Departments of Chemistry, Mechanical, and Aerospace Engineering and Physics, Arizona State University, Tempe, Arizona 85287

ABSTRACT

The kinetics of oxidation of $Ni_{1-y}S_2$ containing ~38, 39, 40, 41.4, and 42 atom percent (a/o) S and NiS were studied at 700° ± 5°C in oxygen at 1 atm. The oxidation of $Ni_{1-y}S_2$ was strongly dependent on its composition. All compositions showed an initial increase followed by a slow decrease in weight. For compositions with 41.4 and 42 a/o S, however, the initial increase in weight was extremely small. Oxidation products of all the compositions were identified by x-ray diffraction as NiO. Oxidation of NiS showed a sharp initial decrease, followed by a slow increase in weight. The oxidation products were identified as Ni_3S_2 and NiO only. The morphology of the oxidized samples was studied using SEM. EDAX was used to identify phases. The possible mechanisms of oxidation are discussed.

Available literature on the phase diagram (1) of the nickel-sulfur system indicates that nickel forms three stable sulfides at 700°C, *viz.*, NiS_2, NiS, and Ni_3S_2. Whereas NiS_2 is almost stoichiometric, NiS and Ni_3S_2 are known to deviate from stoichiometric composition to an appreciable extent. The composition of NiS has been reported to vary from NiS to $NiS_{1.006}$, while that of $Ni_{1-y}S_2$ from $Ni_{2.54}S_2$ to $Ni_{2.66}S_2$ in the temperature range 600°-800°C (1).

The Ni_3S_2 phase is often found as an intermediate corrosion product when nickel is oxidized in sulfur containing gaseous atmosphere (2). High corrosion rates in such atmospheres have been attributed to the presence of this sulfide. Oxidation rates of pure nickel sulfides were, however, not reported in the literature until after completion of the present study. Recently, one paper on this subject has been published by Asaki *et al.* (4). In the present paper, we report results of our studies on the kinetics of oxidation of $Ni_{1-y}S_2$ in pure oxygen at 700°C as a function of its composition. The oxidation of NiS has also been investigated under similar conditions.

Experimental

Five compositions of $Ni_{1-y}S_2$ containing ~38, 39, 40, 41.4, and 42 atom percent (a/o) sulfur were prepared from mixtures containing appropriate proportions of powders of spectroscopic grade nickel, purchased from Johnson-Matthey, and 99.99% pure NiS, purchased from Ventron. These mixtures were sealed in evacuated quartz tubes and then heated at ~700°C for about three days and subsequently near (~20° below) the melting point of the resulting composition for about 12-15h. The capsules were then air quenched to room temperature. The product was ground to a fine powder (~325 mesh) and characterized by x-ray diffraction. No phases other than $Ni_{1-y}S_2$ were detected. The sulfur content of the prepared compounds was confirmed, within ±0.2 a/o, by hydrogen reduction. Cylindrical pellets of ~10 mm diam and 5 mm height were pressed from these powders in a steel die, sintered in evacuated, sealed quartz tubes at ~750°C for three days, and then air quenched to room temperature. The surfaces of these pellets were polished on 4/0 emery paper. Their apparent densities were determined from their dimensions and weights. The total porosity of the sintered pellets varied from ~15% to 25%.

NiS pellets were pressed from as-purchased NiS powder and sintered in evacuated, sealed quartz tubes at ~900°C for 60h. The porosity of these pellets was ~25-30%. The sulfur content of NiS as determined by hydrogen reduction indicated the composition of NiS to be $NiS_{1.006}$.

Oxidation of $Ni_{1-y}S_2$ and NiS pellets was carried out in a flowing stream of oxygen (linear flow rate ~50 cm/min)

* Electrochemical Society Active Member.

3. S. C. Schaefer, U. S. Bureau of Mines RI 8588 (1981).
4. M. Nagamori and T. R. Ingraham, *Metall. Trans.*, **1**, 1821 (1970).
5. F. K. Moghadam and D. A. Stevenson, *J. Appl. Electrochem.*, **13**, 587 (1983).
6. E. T. Turkdogan, "Physical Chemistry of High Temperature Technology," pp. 17, 20, Academic Press, New York (1980).
7. O. Kubaschewski and C. B. Alcock, "Metallurgical Thermochemistry," 5th ed., pp. 300, 331, Pergamon Press, Oxford, England (1979).
8. Y. A. Chang and K. C. Hsieh, Private communication, March, 1984.
9. I. Barin and O. Knacke, "Thermochemical Properties of Inorganic Substances," pp. 579, 648, Springer-Verlag, Berlin (1973).
10. I. Barin, O. Knacke, and O. Kubaschewski, "Thermochemical Properties of Inorganic Substances," Supplement, pp. 460, 467, 600, Springer-Verlag, Berlin (1977).

perature at which the change in slope occurs is extremely sensitive to the terms which correspond to the entropy in the above equations, and hence the errors in the melting temperature are likely to be large. The EMF values obtained from Eq. [1] are in good agreement with those obtained by Schaefer (3) after correcting for the oxygen pressures of the reference electrodes. Our EMF data are also in agreement within ±2 mV with those reported subsequently by Chang and Hsieh (8) for solid $Ni_{3\pm x}S_2$ in the temperature range 945-1070 K.

The virtual cell reaction for cell [A] is

$$Ni_{3\pm x}S_2 + \frac{7\pm x}{2} O_2\,(0.21\ atm) = (3 \pm x)\,NiO + 2SO_2 \quad [3]$$

Therefore

$$\Delta G^\circ_{cell} = 2\Delta G^\circ_{SO_2} + (3 \pm x)\,\Delta G^\circ_{NiO} - \Delta G^\circ_{Ni_{3\pm x}S_2} - \left(\frac{7 \pm x}{2}\right) RT \ln 0.21 \quad [4a]$$

or

$$\Delta G^\circ_{Ni_{3\pm x}S_2} = 2\,\Delta G^\circ_{SO_2} + (3 \pm x)\,\Delta G^\circ_{NiO} - 2F\,(7 \pm x)(E - 0.03362T) \quad [4b]$$

where $\Delta G^\circ_{Ni_{3\pm x}S_2}$, $\Delta G^\circ_{SO_2}$, and ΔG°_{NiO} are the standard Gibbs energies of formation of $Ni_{3\pm x}S_2$, and SO_2, and NiO, respectively, and F is Faraday's constant.

Using the reported data for ΔG°_{NiO} and $\Delta G^\circ_{SO_2}$, one obtains

$$\Delta G^\circ_{Ni_{3\pm x}S_2}(s) = 74{,}740 + 31.007T \pm x\,(-18{,}160 + 11.221T)\ (973\text{-}1089\ K) \quad [5]$$

and

$$\Delta G^\circ_{Ni_{3\pm x}S_2}(l) = -60{,}420 + 17.855T \pm x\,(-16{,}110 + 9.343T)\ (1089\text{-}1173\ K) \quad [6]$$

For the composition of the $Ni_{3\pm x}S_2$ in equilibrium with NiO and SO_2 (1 atm) to be $Ni_{2.666}S_2$ (42.86 a/o S), we obtain

$$\Delta G^\circ_{Ni_{2.666}S_2}(s) = -68{,}670 + 27.257T \quad (973\text{-}1089\ K) \quad [7]$$

and

$$\Delta G^\circ_{Ni_{2.666}S_2}(l) = -55{,}035 + 14.734T \quad (1089\text{-}1173\ K) \quad [8]$$

From Eq. [7] and [8], the enthalpy of fusion of $Ni_{2.666}S_2$ is found to be 13,635 cal/mol.

For the sake of comparison with the data reported in the literature, it is also possible to obtain the Gibbs energy of formation of stoichiometric Ni_3S_2 by assuming the composition in equilibrium with NiO and 1 atm SO_2 to be 40 a/o sulfur. One thus obtains from Eq. [5] and [6]

$$\Delta G^\circ_{Ni_3S_2}(s) = -74{,}740 - 31.007T \quad (973\text{-}1089\ K) \quad [9]$$

and

$$\Delta G^\circ_{Ni_3S_2}(l) = -60{,}420 + + 17.855T \quad (1089\text{-}1173\ K) \quad [10]$$

The enthalpy of fusion of Ni_3S_2, as obtained from Eq. [9] and [10], is 14,320 cal/mol. This is much higher than the estimated value of 5800 cal/mol reported by Kubaschewski and Alcock (7) and is comparable to 11,300 cal/mol reported by Nagamori and Ingraham(4).

Figure 3 shows $\Delta G^\circ_{Ni_{2.666}S_2}$ and $\Delta G_{Ni_3S_2}$, as obtained from Eq. [7]-[10], as functions of temperature. It also shows some of the data reported in the literature. The values of Gibbs energy of formation of solid and liquid Ni_3S_2 obtained from our Eq. [9] and [10] are in good agreement with those reported by Rosenqvist (1) for solid Ni_3S_2 and with those reported by Nagamori and Ingraham (4) for liquid Ni_3S_2. The values of Gibbs energy of formation of solid $Ni_{2.666}S_2$ obtained from our Eq. [7] are also in good agreement with those calculated from Rosenqvist's data in the temperature range 918-1083 K. The enthalpy and entropy terms in our equations are, however, different from those reported by Rosenqvist and by Nagamori and

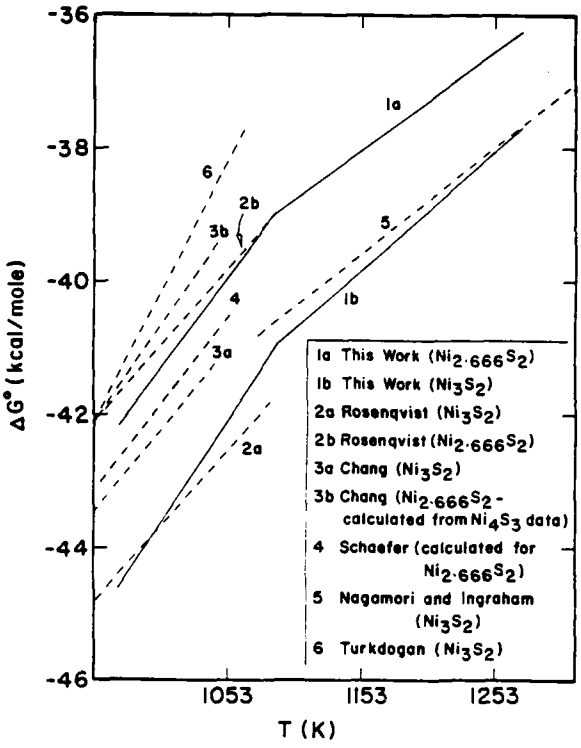

Fig. 3. Standard Gibbs energy of formation of Ni_3S_2 and $Ni_{2.666}S_2$

Ingraham. The agreement between our $\Delta G^\circ_{Ni_{2.666}S_2}$ values and those calculated for the same composition from Schaefer's EMF data is good. The values reported by Lin *et al.* (2) for β_2-Ni_3S_2 (or $Ni_{2.666}S_2$) phase are also in good agreement with those obtained from our Eq. [7]. However, their values for β_1-Ni_3S_2 (40 a/o sulfur) phase are higher than those obtained from our Eq. [9]. The values obtained from the equation for $\Delta G^\circ_{Ni_3S_2}$ (298-1063 K) in Turkdogan's (6) and Kubaschewski and Alcock's (7) compilations, which are actually Rosenqvist's data for the temperature range 673-808 K, are higher by 3-4 kcal/mol than the values obtained in the present work. Because of the very good reproducibility of cell EMF's over the entire temperature range (973-1173 K) and extended durations (4-10 days) of our experiments, and also because of the accuracy of the EMF method itself, the data obtained in the present work may be considered to be more reliable.

Combining the heat capacity data for nickel, sulfur, and Ni_3S_2 reported in literature (7, 9, 10) with the EMF data obtained in this work, one obtains, from the third law analysis, for the enthalpy of formation of Ni_3S_2 from the elements, ΔH°_{298}, a value of −47.9 ± 2.2 kcal/mol. This is in fair agreement with the value of −51.6 ± 2.5 kcal/mol reported by Kubaschewski and Alcock (7). The values of ΔH°_{298} calculated from our EMF data for various temperatures show a random variation and therefore are considered to be free from systematic experimental errors.

Acknowledgments

This research was supported by the Army Research Office under Contract no. DAAG-29-81-K0109 and a grant through the Center for Solid State Science.

Manuscript submitted April 20, 1984; revised manuscript received *ca.* Sept. 11, 1984. This was Paper 429 presented at the Washington, DC, Meeting of the Society, October 9-14, 1983.

Arizona State University assisted in meeting the publication costs of this article.

REFERENCES

1. T. Rosenqvist, *J. Iron Steel Inst.*, **176**, 37 (1954).
2. R. Y. Lin, D. C. Hu, and Y. A. Chang, *Metall. Trans.*, **9B**, 531 (1978).

Experimental Materials and Procedure

Four compositions of $Ni_{1-y}S_2$ containing 38, 40, 42, and 44 atom percent (a/o) sulfur were prepared from 99.999% pure nickel powder (Johnson-Matthey) and 99.99% pure NiS (Alfa/Ventron) or 99.999% pure sulfur. The mixtures, containing appropriate proportions of nickel and NiS powders, or of nickel and sulfur powders, were sealed in evacuated quartz tubes. The sealed ampuls were held at ~970 K for ~72h and subsequently at ~1020-1070 K for 24h, after which they were air quenched. The product was then ground to a fine powder. The chemical compositions of the prepared compounds were verified by reducing them completely in hydrogen. These agreed within 0.3% of the expected sulfur content. Phase identification was done by x-ray diffraction.

Galvanic cells of the scheme

Pt, air ZrO_2 (~Y_2O_3) NiO, $Ni_{1-y}S_2$, SO_2 (1 atm), Pt or Au [A]

were used. One-end closed tubes of yttria-stabilized zirconia, ~7 mm id, purchased from Zirconium Corporation of America, served as the solid electrolyte. Moghadam and Stevenson (5) have reported that the conductivity of partially stabilized YSZ in a SO_2 atmosphere is greater than its conductivity in air and that its ionic transport number is decreased to 0.95-0.67 in the temperature range 773-1273 K by exposure to SO_2. In separate experiments in our laboratory, we have measured the ac conductivity of 9 mole percent (m/o) yttria-stabilized zirconia in air and in flowing SO_2 (1 atm). In the temperature range 873-1273 K, no significant difference in the values of conductivity was observed for this composition of YSZ. This indicates that the electronic transport number of 9 m/o Y_2O_3-ZrO_2 is negligible under our experimental conditions. This is in contrast to the results of Moghadam and Stevenson for yttria-stabilized zirconia containing 4.5 m/o Y_2O_3.

In our experiments, SO_2 was passed over Drierite and P_2O_5. Since, under our experimental conditions, the pressure of SO_2 in equilibrium with SO_3 and O_2 is negligible (8×10^{-13}-3×10^{-11} atm), no correction for SO_3 has been applied and the pressure of SO_2 has been taken to be 1 atm. The open-circuit EMF of cells was measured in the temperature range ~973-1173 K using a Keithley high-impedance multimeter. The temperature of the cell was measured using a Pt-10%Rh/Pt thermocouple.

Results and Discussion

Figure 1 shows the open-circuit EMF as a function of temperature. The results shown are for cells with four different starting compositions of $Ni_{1-y}S_2$ and also with NiS. For each composition, the results were obtained from at least two cells. It can be seen that, irrespective of the starting composition of nickel sulfide, the values of EMF at any given temperature, in the range ~973-1173 K, are identical within the experimental error limits. This suggests that, at a given temperature, the composition of $Ni_{1-y}S_2$ in equilibrium with SO_2 (1 atm) and NiO is fixed and that any other $Ni_{1-y}S_2$ initial composition will convert to this composition. The value of EMF at any temperature remained steady for several hours and was reproducible within ±1 mV during random heating and cooling of the cell, the measurements on which were carried out for a period of up to ten days, and within ±2 mV between independent runs. However, in any run, when the cell was cooled from a temperature above the melting point of Ni_3S_2 to a temperature of ~1000 K or lower, the EMF values obtained were lower than the original values. The values of EMF at temperatures higher than 1000 K could be reproduced any number of times. The values of EMF at temperatures less than ~1000 K could be reproduced in heating and cooling cycles if the cell was not heated to a temperature above ~1073 K.

In order to determine the composition of $Ni_{1-y}S_2$ in equilibrium with SO_2 (1 atm) and NiO at various temperatures, two compositions of $Ni_{1-y}S_2$ containing 38 and 42 a/o sulfur were equilibrated, without NiO present, at ~973, 1073, and 1173 K in a flowing stream of SO_2. These were subsequently analyzed for sulfur using x-ray fluoroescence and gravimetric chemical analysis. The results indicate that the average sulfur content of the $Ni_{1-y}S_2$ is ~42 a/o, although it must be mentioned that the accuracy of these methods for sulfur determination, in the presence of oxygen, was not optimum, the error limits being ±2% a/o sulfur. However, the fact that the EMF values fall on a straight line, in the temperature ranges 973-1089 K and 1089-1173 K, suggests that the variation in the composition of $Ni_{1-y}S_2$ with temperature, if any, is not appreciable. This composition is very close to $Ni_{0.875}S_2$ or Ni_7S_8 (i.e., 42.86 a/o sulfur) which has been suggested to be a stable phase (β_2-Ni_7S_8), in the temperature range 845-1040 K, according to the Ni-S phase diagram reported by Lin *et al.* (2) (shown in Fig. 2). Schaefer (3) has, however, reported that the composition of $Ni_{1-y}S_2$ in equilibrium with NiO and SO_2 (1 atm) is $Ni_{0.91}S_2$ (i.e., 44.3 a/o sulfur). Moreover, he has reported no change in the composition of $Ni_{1-y}S_2$ with temperature in the temperature range (969-1054 K) of his investigation.

The EMF *vs.* temperature relationship has been found to be linear in the present studies. Linear regression analysis of our data in the temperature ranges 973-1053 K and 1083-1173 K yielded the following relationships

$$E = 827.24 - 0.23634T \quad (973\text{-}1089\ \text{K}) \qquad [1]$$

and

$$E = 871.62 - 0.27707T \quad (1089\text{-}1173\ \text{K}) \qquad [2]$$

where E is the EMF of cell [A] in mV and T is the temperature in degrees Kelvin.

The change in the slope of the E *vs.* T straight line at 1089 K corresponds to the melting temperature Ni_3S_2. This is in good agreement with that (1083 K) reported by Rosenqvist and is higher than that (1063 K) reported for Ni_3S_2 by Turkdogan (6), and by Kubaschewski and Alcock (7). However, it must be pointed out that the tem-

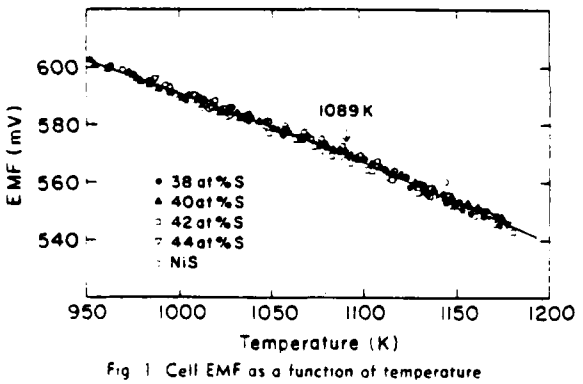

Fig. 1 Cell EMF as a function of temperature

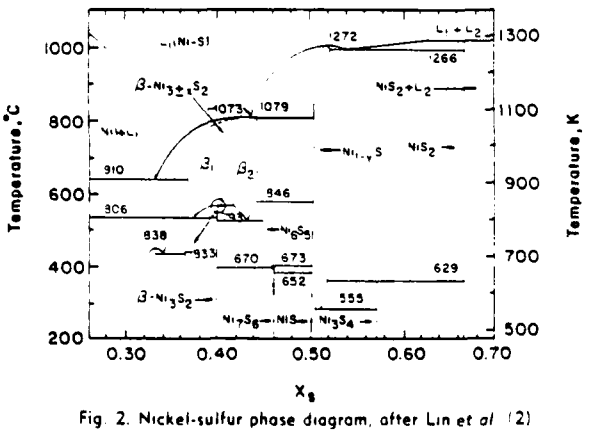

Fig. 2. Nickel-sulfur phase diagram, after Lin *et al.* (2)

Reprinted from JOURNAL OF THE ELECTROCHEMICAL SOCIETY
Vol 132, No. 1, January 1985
Printed in U.S.A.

The Standard Gibbs Energy of Formation of $Ni_{3\pm x}S_2$

G. M. Mehrotra,* V. B. Tare, and J. B. Wagner, Jr.*

Center for Solid State Science, Arizona State University, Tempe, Arizona 85287

ABSTRACT

The standard Gibbs energy of formation of $Ni_{3\pm x}S_2$ has been determined in the temperature range ~973-1173 K using galvanic cells of the configuration,

Pt, air//yttria-stabilized zirconia//NiO, $Ni_{3\pm x}S_2$, SO_2 (1 atm), Pt or Au

In the temperature range of the investigation, the open-circuit EMF of the cell, at any given temperature, was found to be independent of the starting composition of $Ni_{3\pm x}S_2$ within the experimental error limits. With the composition of $Ni_{3\pm x}S_2$ in equilibrium with NiO and SO_2 (1 atm) being $Ni_{2.666}S_2$, the results in calories per gram mole are

$$\Delta G^\circ_{Ni_{2.666}S_2}(s) = -68{,}670 + 27.257T \text{ (973-1089 K)}$$

$$\Delta G^\circ_{Ni_{2.666}S_2}(l) = -55{,}035 + 14.734T \text{ (1089-1173 K)}$$

The temperature and enthalpy of fusion of $Ni_{2.666}S_2$ are, therefore, 1089 K and 13,635 cal/mol, respectively. For the stoichiometric Ni_3S_2, we obtained

$$\Delta G^\circ_{Ni_3S_2}(s) = -74{,}740 + 31.007T \text{ (973-1089)}$$

$$\Delta G^\circ_{Ni_3S_2}(l) = -60{,}420 + 17.855T \text{ (1089-1173)}$$

The enthalpy of fusion of Ni_3S_2 is 14,320 cal/mol.

The thermodynamics of nickel sulfides has been the subject of several investigations. Rosenqvist (1) studied the $NiS_x/H_2S/H_2$ equilibria and reported thermodynamic data for solid Ni_3S_2, Ni_6S_{5+x}, Ni_7S_6, NiS_{1+x}, and NiS_2 compounds. Lin *et al.* have also studied the nickel-sulfur system, in the temperature range 823-1023 K, using a gas equilibration technique. More recently, Schaefer (3) has carried out electrochemical determination of the free energy of formation of solid $Ni_{2+x}S_2$ phase. Nagamori and Ingraham (4) have investigated the nickel-sulfur melts by measuring the equilibrium weight of the melt in gas streams of H_2 and H_2S and have reported the standard Gibbs energy of formation of liquid Ni_3S_2 and liquid NiS. However, there appears to be no thermodynamic investigation over a wide temperature range covering both solid as well as liquid $Ni_{3\pm x}S_2$. Moreover, the data obtained by various investigators separately for solid and liquid Ni_3S_2 do not yield consistent values for temperature and enthalpy of fusion of Ni_3S_2. In the present work, the thermodynamics of solid and liquid $Ni_{3\pm x}S_2$ have been studied using solid electrolyte galvanic cells in the temperature range ~973-1173 K.

*Electrochemical Society Active Member.

tion of Ni_3S_2 the current carriers are electrons. Above 10 mole % Ni_3S_2 the volume fraction of the Ni_3S_2 particles becomes so large that continuous contact between Ni_3S_2 particles becomes possible and hence metallic type of conduction corresponding to pure Ni_3S_2 is observed. Evidence for the continuous migration paths is provided by the micrographs shown in Fig. 3(c).

It is relevent to comment on the existing hypothesis put forward to explain the effect of a dispersed conducting phase in a semiconducting matrix.

Wagner[12] calculated the concentration of electrons and hence the resulting conductivity of oxides with inclusion of spherical metallic particles by introducing a concept of a space charge layer at the interface. However, in estimating these concentrations a complete thermodynamic equilibrium is assumed. In many practical cases, systems are far from equilibrium, particularly if the temperatures are low, as in the present study. Hence the applicability of this model is restricted.

In describing conduction in homogeneous media Landaur[13] and Bergman[14] discussed the percolation model for conduction in a semiconductive or insulating medium containing small metallic particles as the dispersed phase. The theory is based mainly on geometrical considerations and does not take into account the nature and the concentration of current carriers. Approximately at a volume fraction between 10%–15% a continuous network of a highly conducting dispersoid is expected to form, resulting in a high apparent total conductivity. Very little change in conduction is expected below this threshold concentration known as percolation threshold. In the present context, an explanation involving percolation appears to be inadequate because the conductivity shows a minimum at 5 mole % Ni_3S_2 in NiO. Moreover, no percolation threshold is observed.

It has been mentioned earlier that the corrosion product of nickel in sulfur containing atmosphere is often found to consist of Ni_3S_2 dispersed in NiO. The present investigations indicate that to have fast transport through Ni_3S_2 a conducting network of Ni_3S_2 must be present. This can happen only when the concentration of Ni_3S_2 exceeds 10 mole % or 30 vol %. This is in agreement with the data reported by Luthra and Worrell[4] who observed that the corrosion product of nickel consists of approximately 50 vol % of Ni_3S_2. Under certain experimental conditions, particularly at low sulfur potentials and higher temperatures, lower concentration of Ni_3S_2 has been observed. Under such conditions the kinetics of corrosion are expected to be governed by the transport through the composites which will be essentially controlled by the nonequilibrium concentration of point defects which in turn are related to the electronic defects and will be strongly dependent upon whether the concentration of Ni_3S_2 is greater or lower than 5 mole % (16 vol %) Ni_3S_2. As yet there are no reports on corrosion rates as a function of sulfide content. Their lack may be one source of disagreement in the reported kinetics.

ACKNOWLEDGMENT

This research was initiated under the Army Research Office, Contract No. DAAG 29-81-K-0109 and subsequently funded by a grant from Center for Solid State Science, Arizona State University.

[1] J. B. Wagner, Jr., Mater. Res. Bull. 15, 1691 (1980).
[2] M. H. Cohen, J. Jortner, and I. Webman, "Electrical Transport and Optical Properties of Inhomogeneous Media," AIP Conference Proceedings, September 7–9, 1977 (American Institute of Physics, 1978), edited by J. C. Garland and D. B. Tanner, pp. 63–83.
[3] C. S. Giggins and F. S. Petit, Oxid. Met. 14, 363 (1980).
[4] K. L. Luthra and W. L. Worrell, Metall. Trans. A 9, 1055 (1978), *ibid.* 10, 621 (1979).
[5] ASTM-X-Ray Diffraction Data Cards.
[6] R. Y. Lin, D. C. Hu, and Y. A. Chang, Metall. Trans. B 9, 531 (1978)
[7] C. M. Osburn and R. W. Vest, J. Phys. Chem. Solids 32, 1331 (1971), and 32, 1343 (1971).
[8] N. G. Eror and J. B. Wagner, Jr., Phys. Status Solidi 35, 641 (1969).
[9] M. C. Pope and N. Birks, Oxid. Met. 12, 191 (1978).
[10] S. P. Mitoff, J. Chem. Phys. 35, 882 (1961).
[11] H. Yagi and J. B. Wagner, Jr., Oxid. Met. 18, Nos. 1/2, 39 (1982).
[12] C. Wagner, J. Phys. Chem. Solids 33, 1050 (1972).
[13] R. Landaur, "Electrical Transport and Optical Properties of Inhomogeneous Media," AIP Conference Proceedings, Sept. 7–9, 1977 (American Institute of Physics, 1978), edited by J. C. Garland and D. B. Tanner, p. 2.
[14] D. J Bergman, "Electrical Transport and Optical Properties of Inhomogeneous Media," AIP Conference Proceedings, Sept. 7–9, 1977 (American Institute of Physics, 1978), edited by J. C. Garland and D. B. Tanner, p. 46.

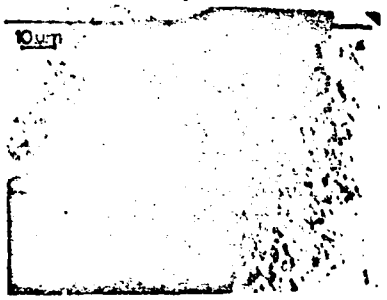

FIG. 6. Ni_3S_2 particle in NiO matrix.

the same temperature range but measured at $10^{-0.013}$ atmospheres of oxygen. The activation energy of 12.9 kcal/mole reported by them is very close to 13.11 ± 0.77 kcal/mole obtained from the present data. A value of 13 kcal/mole was also reported by Eror and Wagner[8] for the activation energy for the movement of electron holes for NiO single crystals at 9.4×10^{-3} atmospheres of oxygen pressure. At high temperatures (> 1000 °C) where the samples are both in thermal and chemical equilibrium, an activation energy of 22–23 kcal/mole has been reported.[7,8] Because the present data are limited to only 800 °C a comparison is not possible. However, a tendency towards higher activation energy is indicated at higher temperatures by the deviation from the linear behavior.

Since the samples used in present investigations were prepared from NiO powder equilibriated in air at high temperatures and the fact that the sintering temperature and the temperature range of measurement were only 600–800 °C, the high values of conductivities and low values of activation energy are most probably due to the nonequilibrium between the sample and the surrounding oxygen partial pressure which approximately corresponds to Ni-NiO equilibria. It has been shown by Osburn and Vest[7] that the equilibria between NiO and oxygen is extremely sluggish at low temperatures.

The activation energies of conduction obtained in the present investigation can therefore be considered to be the activation enthalpies of migration of electron holes with the defect equilibria given by Eqs. (1) and/or (2) above. Under equilibrium conditions the concentration of holes and hence the electrical conductivity will be directly proportional to the oxygen pressure to an exponent $1/n$. However, if the equilibration is slow, as is the case at lower temperatures, one would still expect higher conductivity corresponding to the defect equilibria present at higher temperature.

Addition of sulfur to the NiO lattice decreases the conductivity of NiO indicating the decrease in the concentration of mobile holes. The solubility of sulfur in NiO, although small, is reported to be $10^{-2}\%$–$10^{-3}\%$.[9] If the sulfur is assumed to occupy normal lattice site of oxygen, the defect equilibria may be modified as

$$\tfrac{1}{2}S_2 + O_0 + \oplus = \dot{S}_0 + \tfrac{1}{2}O_2 \text{ or } \tfrac{1}{2}S_2 + O_0 + 2\oplus = \ddot{S}_0 + \tfrac{1}{2}O_2,$$

where S replaces oxygen from lattice either as singly charged ion or neutral atom. In either case the concentration of holes and hence the conductivity will decrease. Sulfur can also replace oxygen as negatively charged sulfur ion with 2 negative charges. In such a case no change in conductivity is expected. The observed change in conductivity is, however, too small to justify unambiguously the modification of defect structure as proposed above. It is, however, also possible that because of lower temperatures the above reaction is also very slow and does not go to completion.

The decrease in conductivity on adding > mole % Ni_3S_2 to NiO is, however, more dramatic. The activation energy of conduction also increases appreciably.

Conduction in pure Ni_3S_2 has been reported to be metallic.[11] The presence of Ni_3S_2 as a dispersed phase is therefore suspected, in some way, to bind locally the mobile holes contributing to conduction. It may be noted that because the concentration of holes in nickel oxide is already higher than the equilibrium concentration due to the metastable defect equilibria, the electrons provided by nickel sulfide at the NiO-Ni_3S_2 interface combine with the holes creating a condition which is closer to the equilibrium and hence energetically more stable. Such a possibility was first considered by Eror and Wagner[8] who postulated that if the concentration of electronic carriers is low, it is likely that large numbers of them get trapped by some type of imperfection that is not considered in the conventional theory of point defects. One type of imperfection was considered by them to be dislocations. In the present context it is suggested that such trapping sites are provided by the NiO-Ni_3S_2 interface which make the trapping of carriers even easier because of the opposing nature of carriers in NiO and Ni_3S_2. The overall effect will be to reduce the number of mobile carriers and hence the conductivity. There will, however, be a definite equilibria associated with this electron hole pair and hence the number of mobile carriers will be strongly dependent on the temperature. The observed increase in the activation energy is consistent with this view.

When most of the mobile holes are trapped in this way, further change in conductivity is considered to be due to the predominant concentration of electrons from the increased concentration of Ni_3S_2. This is also evident from the observation that compositions containing increasing concentra-

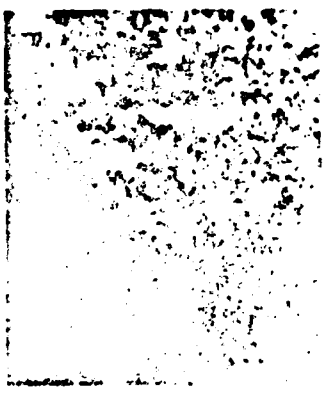

FIG. 7. SEM image showing NiO-Ni_3S_2 interface

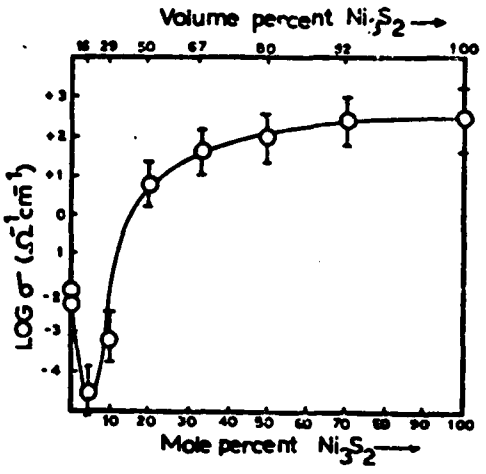

FIG. 2. Electrical conductivity as a function of composition of NiO–Ni_3S_2 mixtures at 600 °C.

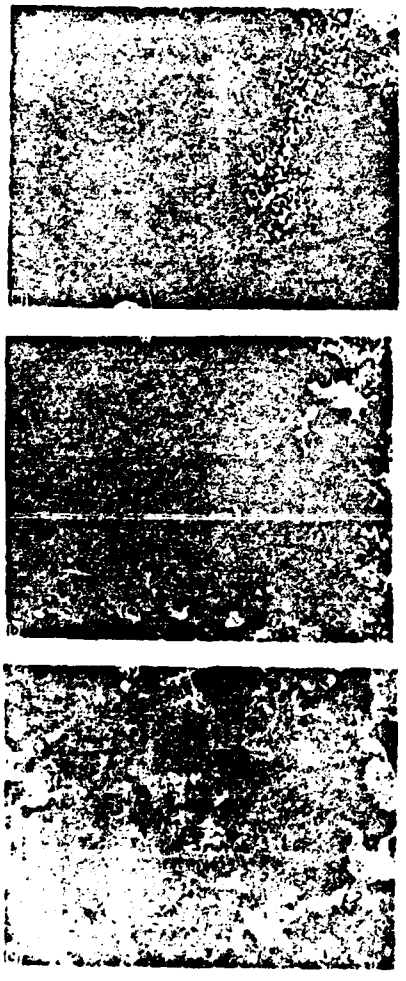

FIG. 3. SEM image showing the distribution of Ni_3S_2 in NiO. (a) 5 mole % Ni_3S_2, (b) 10 mole % Ni_3S_2, (c) 20 mole % Ni_3S_2. Distribution of Ni_3S_2 is random in 5 mole % and 10 mole % Ni_3S_2, while continuous network of Ni_3S_2 in 20 mole % Ni_3S_2 is clearly seen.

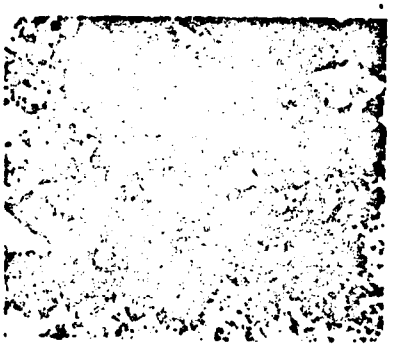

FIG. 4. SEM image of the nickel oxide matrix at higher magnification. Arrows show the presence of pores.

NiO is found to be higher compared to the value reported in the literature for single crystalline as well as polycrystalline samples.[7,8] Conductivity of NiO as a function of temperature and oxygen pressure has been widely investigated. Comparison of the data, however, becomes difficult because of the widely differing conditions used by various investigators. Similarly, the conductivity is very sensitive to the type and amount of impurities present. For substances having low impurity levels as in the present case, if there is complete thermal and chemical equilibrium, the disorder in NiO can be satisfactorily explained by the two equilibria:

$$\tfrac{1}{2}O_2 \rightleftarrows O_O + V'_{Ni} + \oplus, \quad (1)$$

$$\tfrac{1}{2}O_2 \rightleftarrows O_O + V''_{Ni} + 2\oplus. \quad (2)$$

Accordingly, either $P_{O_2}^{1/4}$ or $P_{O_2}^{1/6}$ pressure dependence of conductivity is obtained. These equations are written using the usual Kröger and Vink notation. From the variation of conductivity with temperature at fixed oxygen pressures, Mitoff[9] obtained two activation energies. The lower activation energy obtained at lower temperature was attributed to the lack of thermodynamic equilibrium implying little change in the composition of the sample. The activation energy for conduction under these conditions would reflect only the activation enthalpy for movement of electron holes.

Data obtained in the present investigation are compared in Fig. 1 with those obtained by Osburn and Vest[7] in

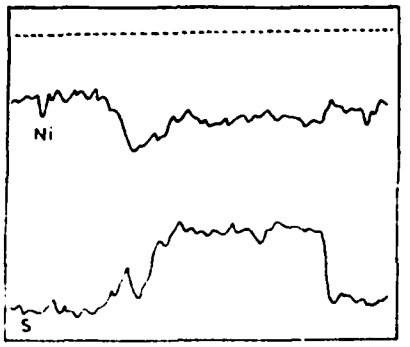

FIG. 5. Concentration profile of Ni and S across the Ni_3S_2 particle shown in Fig. 6.

TABLE I. Measured and theoretical densities and percent porosities of various NiO–Ni_3S_2 compositions.

S.N.	Mole% Ni_3S_2	Vol% Ni_3S_2	Density[a] (theoretical)	Density (measured)	% Porosity
1	0	0	6.67	4.48	32.83
2	~0	~0	6.67	4.50	32.53
3	5	16	6.55	3.80	41.98
4	10	29	6.45	4.20	34.88
5	20	50	6.29	4.43	29.57
6	33.3	67	6.24	4.41	29.32
7	100	100	5.82	5.75	1.2

[a] Density of pure NiO = 6.67 g/cm^3 and pure Ni_3S_2 = 5.82 g/cm^3 (Ref. 5).

dominant current carriers were found to be electron holes, while for 5 mole % and higher concentration of Ni_3S_2 the predominant current carriers were determined to be electrons.

Scanning electron microscopic examination of the various compositions (Fig. 3), shows that Ni_3S_2 particles are distributed in NiO matrix fairly uniformly. The particle size of Ni_3S_2 varies from 10 to 100 μm with the average around 75 μm. Figure 4 also is a micrograph with higher magnification for samples containing 5 mole % Ni_3S_2 of the region where only NiO is believed to be present. NiO grains are of uniform size of approximately 5 μm. The number of pores, the evidence for which was obtained from the measured densities, is also clearly seen. The average size of the pores is also $\simeq$5 μm. The microscopic examination also reveals that the dispersed Ni_3S_2 particles have random, irregular shapes. The needle-type growth as reported by other investigators during corrosion of nickel in sulfur dioxide is clearly absent. Figure 3(c) shows the SEM picture of sample containing 20 mole % Ni_3S_2 which shows very high metallic-type conductivity. The Ni_3S_2 particles are seen to form a continuous network indicating that conduction is mostly through interconnected nickel sulfide particles. This continuous network of Ni_3S_2 is also seen in the fractured sample surface perpendicular to the cylindrical axis of the pellet.

The concentration profile of nickel and sulfur was obtained by EDAX across a selected cross section shown in Fig. 6. The profile is shown in Fig. 5. The concentration of nickel at the beginning corresponds to that in NiO. There is a visible decrease in concentration as one crosses the Ni_3S_2 particle. This decrease is associated with the increase in concentration of the sulfur confirming the presence of sulfide particles. At interfaces of NiO and Ni_3S_2 particles the concentration of nickel as well as sulfur decreases simultaneously suggesting the possibility of the existence of a void of approximately 5 μm in width. The presence of small voids is also evident from Fig. 7, which shows a highly magnified image of the interface. Voids of these dimensions are also visible at the interface of NiO grains (Fig. 4). One can therefore conclude that the interfacial contact between NiO and Ni_3S_2 is as good as the contact between nickel oxide grains.

X-ray diffraction patterns of all the compositions taken before and after the conductivity measurements were found to be identical, confirming the presence of only two phases, viz. NiO and Ni_3S_2. In spite of careful examination by SEM, EDAX, and x rays, there was no evidence of the presence of nickel as a third phase. Formation of Ni by the disproportion reaction of Ni_3S_2 at temperatures below 600 °C was reported by Luthra and Worrell.[4]

Formation of metallic nickel in the temperature range of measurement of conductivity, by the reaction

$$NiO + Ni_3S_2 = Ni + SO_2$$

is thermodynamically feasible, particularly at low sulfur-dioxide partial pressures. There is no evidence for the occurrence of this reaction under the present experimental conditions. Similarly separate experiments showed that the oxidation of Ni_3S_2 is slow even in pure oxygen and almost absent in purified argon. Because of these reasons the change in concentration of Ni_3S_2 under the present conditions of experiment is believed to be improbable.

The absolute value of the specific conductivity of pure

TABLE II. Expressions for temperature dependence of conductivity and the activation energies of conduction for various samples in the temperature range 873–1073 K.

	Composition	$\log \sigma = a + \frac{b}{T}$	Activation energy kcal/mole
1	Pure NiO	$1.27 - \frac{2876}{T}$	13.11 ± 0.77
2	NiO saturated with S	$1.43 - \frac{3261}{T}$	14.86 ± 0.73
3	NiO + 5 mole% Ni_3S_2	$3.31 - \frac{6380}{T}$	29.09 ± 1.00
4	NiO + 10 mole% Ni_3S_2	$2.13 - \frac{4683}{T}$	21.35 ± 2.05

silica tube in which a continuous flow of argon, purified by passing it over Drierite, copper turnings heated at 400 °C and phosphorous pentoxide, was maintained. To decrease the oxygen content of the gas surrounding the sample still further, the gas was passed over nickel foil kept very near the sample. The whole assembly was inserted in a Kanthal wound furnace, the temperature of which was controlled to within ± 1 °C by a proportional controller. The platinum wires spot welded to the two platinum foils in which the sample pellet was sandwiched, acted as leads for measuring resistance and a Pt-Pt + 10% Rh thermocouple kept very near the sample measured the temperature to ± 0.1 °C.

Specific conductivity was estimated from the measured resistance by using the usual relationship $\sigma = l/RA$, where σ is specific conductivity in $\Omega^{-1}\,cm^{-1}$, l the distance between two platinum electrodes measured in terms of thickness of pellets in centimeters, A the area of contact in cm^2 calculated from the diameter of the pellet, and R in Ω measured by the bridge. Measurements were carried out on at least two different pellets of the same compositions to test reproducibility. The temperature range of measurement was restricted to 600°–800 °C. The higher temperature limit of 800 °C was because of the reported melting of Ni_3S_2 above this temperature and lower temperature limit of 600 °C was because of the crystalline transformation and possible disproportionation reaction.[6]

(d) Determination of the nature of current carriers: To obtain qualitative information about the predominant current carriers, pellets were kept between two silver blocks, one of which was heated by means of a soldering iron. The direction of the current was observed using a Keithley Electrometer. For predominant electrons as current carriers (*n*-type semiconductors) the hot end becomes positive, while for predominant positive holes as current carriers (*p*-type semiconductor) it becomes negative.

(e) Characterization of samples: X-ray diffraction patterns of all the samples were obtained after the conductivity measurements were complete. Similarly, samples were examined optically after polishing the faces again. Samples were also examined under Scanning Electron Microscope JEOL JSM35 type to obtain morphological details. The concentration profile of nickel as well as sulfur was obtained using Energy Dispersive Analysis of x rays.

III. RESULTS AND DISCUSSION

Variation of $\log \sigma$ with $1/T$ is shown in Fig. 1 for various samples. At least two or three independent measurements were obtained for each composition. The data presented in Fig. 1 include results of all samples investigated. The scatter for compositions containing 5 mole % Ni_3S_2 and 10 mole % Ni_3S_2 appears to be large. This may be due to the lack of equilibrium between the samples and the ambient atmosphere. Compositions containing greater than 10 mole % Ni_3S_2 show a very high conductivity which decreases slightly with increase in temperature, a behavior typical of metallic conduction. For these compositions, therefore, conductivity only at 600 °C has been obtained. Because of the very high conductivity and insensitivity of measuring instruments to such high conductivities, the error margin for these compositions is relatively large.

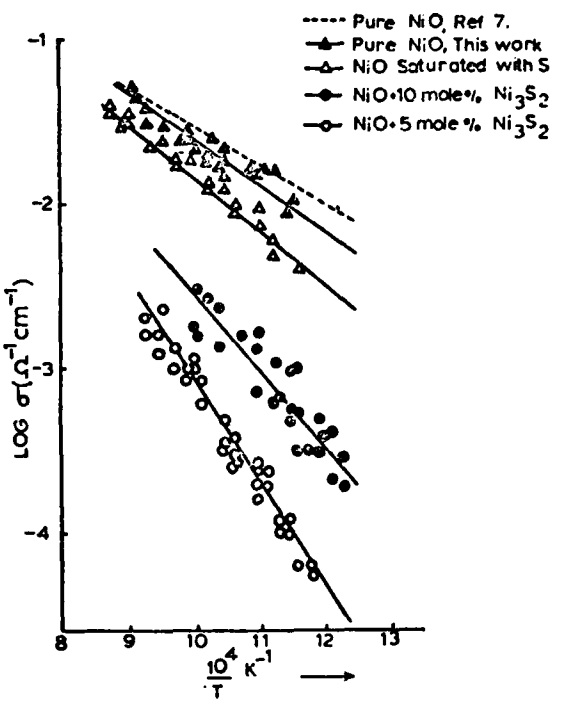

FIG. 1. Electrical conductivity as a function of reciprocal temperature for various NiO–Ni_3S_2 compositions.

Table I gives the calculated and observed densities and percentage porosity for all the compositions which are shown both in mole % as well as volume percent.

Table II gives the expressions obtained by linear regression analysis of the data shown in Fig. 1. Activation energies of conduction have also been obtained using an Arrhenius type relation and are shown in Table II with the respective standard deviations.

The specific conductivity is shown in Fig. 2 as a function of concentration of Ni_3S_2 shown both as mole % as well as volume percent at 600 °C. For samples saturated with sulfur the conductivity is found to decrease slightly as compared to pure NiO. Significant decrease in conductivity is observed for samples containing 5 mole % Ni_3S_2. Increasing the concentration of Ni_3S_2 above 5 mole % increases the conductivity as seen for samples containing 10 mole % Ni_3S_2. The conductivity, however, increases with increase in temperature indicating that the semiconducting behavior is still maintained. For the samples containing higher concentrations of Ni_3S_2, however, the conductivity increases sharply and becomes metallic; i.e., the conductivity decreases with the increase in temperature.

The apparent activation energy of conduction also follows the same pattern viz. the value increases with increased concentration of Ni_3S_2, attains a maximum (29.1 kcal/mole) at approximately 5 mole % Ni_3S_2, and then decreases again with the increase in the concentration of Ni_3S_2.

For pure NiO and NiO saturated with sulfur, the pre-

ARO 18043.2-MS

Electrical conduction in two-phase nickel oxide-nickel sulfide mixtures

V. B. Tare and J. B. Wagner, Jr.
Center for Solid State Science, Arizona State University, Tempe, Arizona 85281

(Received 30 July 1982; accepted for publication 4 October 1982)

The electrical conductivity of sintered pellets of NiO-Ni_3S_2 mixtures of various compositions has been measured as a function of temperature in the range 600–800 °C. The electrical conductivity of pure nickel oxide initially heated in known sulfur vapor at 950 °C for 100 h has also been measured as a function of temperature. The conductivity of NiO-Ni_3S_2 decreases initially, attains a minimum at approximately 5 mole % Ni_3S_2 and increases again with an increase in concentration of Ni_3S_2. The activation energy for conduction also follows the same pattern. The conductivity changes from predominantly *p* type for pure and sulfur saturated NiO to predominantly *n* type for compositions equal to or greater than 5 mole % Ni_3S_2. The results have been explained by postulating the trapping of holes at the NiO-Ni_3S_2 interface by the electrons from Ni_3S_2. At concentrations higher than or equal to 20 mole % Ni_3S_2 the conduction is predominantly due to electrons from the Ni_3S_2 phase. The morphological details of the NiO-Ni_3S_2 composites have been obtained using scanning electron microscopy. The concentration profiles of nickel and sulfur across the composite were obtained by using Energy Dispersive Analysis of x rays.

PACS numbers: 72.80.Ga

I. INTRODUCTION

Electrical transport in multiphase systems, because of their unusual electrical properties, has received the attention of several investigators recently. It has been reported, for example, that the dispersion of an insulating phase in an electrolyte matrix increases electrical transport by several orders of magnitude.[1] The enhancement with increasing concentration of dispersoid has been found to be continuous. On the other hand, a dispersion of metallic particles in a semiconducting or insulating matrix is believed to result in a critical concentration of dispersoid giving rise to nonmetal-metal transition.[2] Very little information is available, however, regarding the effect of a highly conducting compound dispersed in a semiconductor. One often encounters such a situation in a two-phase mixture of sulfide and oxide formed as a result of the corrosion of metals in environments containing both sulfur and oxygen.[3] More specifically, when metallic nickel is exposed to an oxygen atmosphere containing sulfur dioxide, corrosion products, under certain conditions, are found to contain nickel oxide as well as nickel sulfide.[4] The presence of nickel sulfide was suspected to be the main reason for the very high corrosion rates. Because corrosion is often related to transport through the product layer, the present investigation describes the effect of varying concentration of Ni_3S_2 on the electrical conductivity of NiO.

II. EXPERIMENTAL

(a) Materials used: Nickel Oxide (NiO) powder of approximately −300 mesh and of Johnson Matthey Puratronic grade (99.999% pure) was purchased from Alfa Division Ventron Corporation. The nickel oxide powder was heated in air at 1000 °C for 24 h in order to fix the composition and to sinter the material prior to pressing. The initial particle size was $\approx 1\,\mu m$ and final particle size prior to pelletizing was about 5 μm. Nickel Sulfide (Ni_3S_2) was prepared from nickel powder and nickel monosulfide (NiS) also of the same grade. These powders were thoroughly mixed in proportions such that the mixture corresponded to stoichiometric Ni_3S_2. The mixture was heated in an evacuated ($\approx 10^{-3}$ Torr) sealed silica capsule for 24 h at 600 °C followed by 4 h at 800 °C. The resulting product was air quenched to room temperature, ground to a fine powder with an average particle size of 75 microns, and examined by x-ray diffraction. No phase other than Ni_3S_2 was detected.

Sulfur-saturated NiO was prepared by heating a compressed pellet of NiO powder in sulfur vapor of $\sim 10^{-3}$ Torr obtained by heating elemental sulfur at $\approx$80 °C in a previously evacuated silica tube at 950 °C for 150 h.

(b) Sample preparation: Pellets of NiO were prepared by pressing the powder in a steel die of $\approx$12 mm diameter under hydrostatic pressure of 5 tons/sq. in. Pellets of various compositions of NiO and Ni_3S_2 were also prepared by mixing these powders in appropriate proportions and pressing them under similar conditions. All the pellets were sintered at 750 °C for 24 h after encapsulating them in a nickel foil and sealing them in an evacuated silica tube. This precaution was necessary to avoid any oxidation of Ni_3S_2.

After sintering, the pellets were lightly polished on 4/0 emery paper. The dimensions of pellets were measured using a micrometer to within $\pm$ 0.001 mm. The weights were measured to a hundredth of a milligram. Geometrical densities were estimated from these dimensions and compared with the one calculated from the data reported in the literature[5] for pure NiO and pure Ni_3S_2 to obtain the apparent porosity of the pellets.

(c) Measurement of electrical conductivity: The ac electrical conductivity of the pellets was obtained by measuring their resistance at 1 kHz with a resistance bridge using the two-probe method. Platinum paste was applied to the polished faces of the pellet to ensure good electrical contact. Pellets were pressed between two platinum foils in a spring-loaded silica assembly. The assembly was kept in another

 0021-8979/83/010252-06$02.40

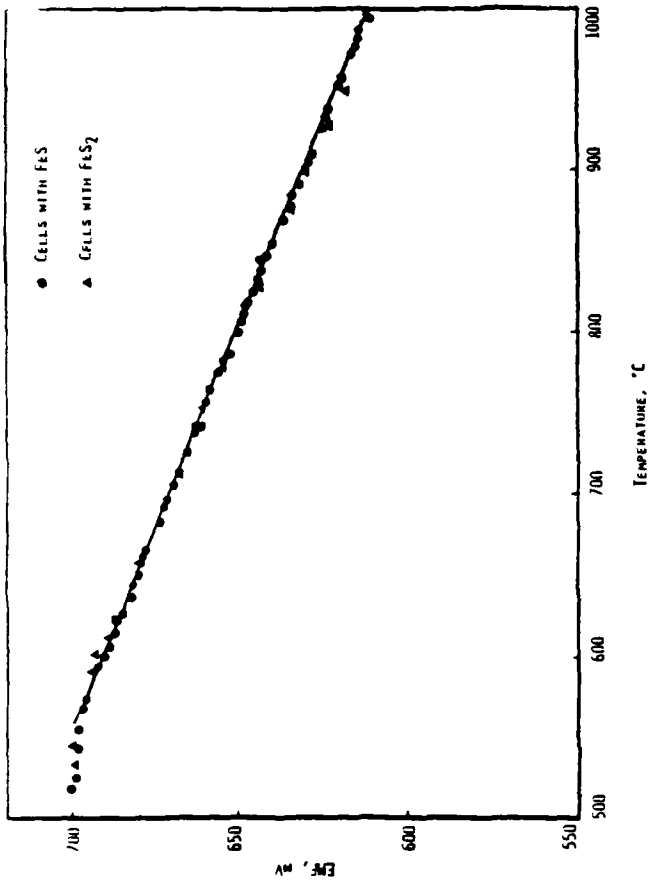

Figure 1. EMF of cell (A) as a function of temperature.

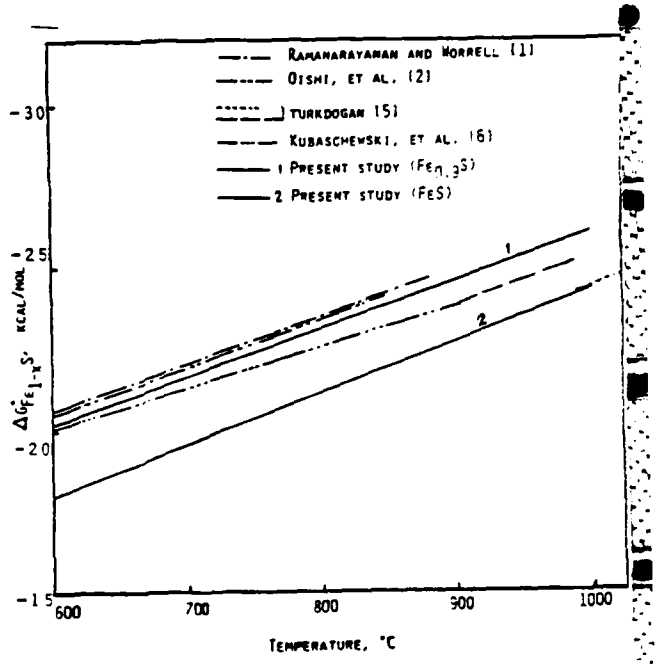

Figure 2. Standard Gibbs energy of formation of F

Asaki *et al.* (3, 4) suggested that, during initial stages of oxidation of FeS or Ni_3S_2, diffusion through sulfide may control the overall rate of oxidation. Yagi and Wagner (5) studied the chemical diffusivity in $Ni_{1-y}S$ as a function of composition and showed that, although there is a small compositional dependence of diffusivity, the diffusivity values for all the compositions are very high. The concentration gradients in Ni_3S_2 throughout its oxidation may, therefore, be regarded as negligibly small.

The oxidation reaction leading to the formation of SO_2 and NiO may take place either at NiO/O_2 interface or at Ni_3S_2/NiO interface. The former requires transport of nickel and sulfur through a compact NiO layer. This is extremely slow and may be the cause of the observed negligibly small rates of oxidation of nickel sulfide containing 39 a/o S. For all the other compositions, because of the presence of cracks in the nickel oxide layer formed, oxygen can migrate through the cracks and react with nickel sulfide at the NiO/Ni S interface forming fresh NiO and SO_2, which is again carried away by the diffusion through cracks in NiO. The rate is thus governed by either the diffusion of O_2 or of SO_2 through crac[illegible] in NiO. It is surprising, however that even after [illegible] of oxidation only 25% of the reaction is complete. The rate after this period becomes extremely slow. This suggests that the number and/or size of cracks present in NiO are likely to be very small.

Unlike Ni_3S_2, the oxidation of NiS at 7[illegible] C in oxygen exhibits a very fast initial weight loss within the first 10 min, followed by a weight gain, the rate of which becomes so small that the oxide formed offers virtual protection against further oxidation. X-ray and EDAX indicated the presence of NiO and Ni S phases only.

The initial oxidation of NiS may be represented by

$$(3 \pm x)NiS + (1 \pm x)O_2 = Ni_{1\pm x}S_2 + (1 \pm x)SO_2 \quad [4]$$

or

$$(4 \pm x)NiS + (2.5 \pm x)O_2 = Ni_{1\pm x}S_2 + NiO + (2 \pm x)SO_2 \quad [5]$$

Once the $Ni_{1\pm x}S_2$ is formed, subsequent oxidation takes place by the mechanisms discussed above. The subsequent slow rate of oxidation suggests that nickel sulfide with either 39 or 40 a/o S is probably formed as the intermediate oxidation product. However, from the observed fractional weight loss in the initial stage, it seems that nickel sulfide containing ~42.7 a/o sulfur is formed.

Acknowledgments

This research was supported by The Army Research Office under Contract no. DAAG29-81-K-0109 and a grant from the Center for Solid State Science.

Manuscript submitted March 26, 1984; revised manuscript received *ca.* Sept. 11, 1984. This was Paper 463 presented at the San Francisco, California, Meeting of the Society, May 8-13, 1983.

Arizona State University assisted in meeting the publication costs of this article.

REFERENCES

1. R. Y. Lin, D. C. Hu, and Y. A. Chang, *Metall. Trans.*, **9B**, 531 (1978).
2. K. L. Luthra and W. L. Worrell, *ibid.*, **9A**, 1055 (1978).
3. Z. Asaki, K. Matsumoto, T. Tanabe, and Y. Kondo, *ibid.*, **14B**, 109 (1983).
4. Z. Asaki, K. Hajika, T. Tanabe, and Y. Kondo, *ibid.*, **15B**, 127 (1984).
5. H. Yagi and J. B. Wagner, Jr., *Oxid. Met.*, **18**, 42 (1982).

Oxidation of Metals, Vol. 18, Nos. 1/2, 1982

Chemical Diffusion and Electrical Conductivity of $Ni_{3\pm x}S_2$

H. Yagi and J. B. Wagner, Jr.*

Received April 27, 1982

The sulfur activity-composition relation of β-$Ni_{3\pm x}S_2$ was determined between 600 and 750°C by thermogravimetry using H_2S/H_2 gas mixtures. The existence of β_1- and β_2-$Ni_{3\pm x}S_2$ was confirmed. The chemical diffusion coefficient of β-$Ni_{3\pm x}S_2$ was measured as a function of composition at 650°, 700°, and 750°C using thermogravimetry for the reequilibration reaction. The chemical diffusion coefficients varied with composition and showed a maximum at stoichiometric composition, Ni_3S_2. The activation energy for chemical diffusion was determined as $E_a = 31.3$ Kcal·mole^{-1} for stoichiometric Ni_3S_2. Electrical conductivity of β-$Ni_{3\pm x}S_2$ was determined as a function of composition at 650°C. The electrical conductivity increased with increasing the mole fraction of sulfur. The temperature dependence of the electrical conductivity of Ni_3S_2 was measured between 50 and 750°C and found to exhibit metallic behavior.

KEY WORDS: Nickel sulfide; activity; chemical diffusion; electrical conductivity; thermodynamics.

INTRODUCTION

$Ni_{3\pm x}S_2$ has often been found as the reaction product in nickel corrosion in pure SO_2 or SO_2–O_2 gas mixtures at elevated temperatures.[1-3] The rates of the reaction of nickel in these gas mixtures are extremely rapid. For example, the corrosion rates of nickel in SO_2–O_2 atmospheres at 603°C are 10^5–10^6 times faster than the rate of oxidation of nickel in oxygen at 1 atm[3]. These rapid rates have often been explained by possible rapid diffusion of nickel through continuous nickel sulfide channels ($Ni_{3\pm x}S_2$) formed within nickel oxide scale.[2,3] However, knowledge of the transport properties of $Ni_{3\pm x}S_2$ phase is very limited.

The homogeneity range of high temperature $Ni_{3\pm x}S_2$ phase in the nickel–sulfur system has been studied by various investigators.[4-8] Lin *et*

*Center for Solid State Science, Arizona State University, Tempe, Arizona 85287.

0030-770X/82/0800-0041$03.00/0

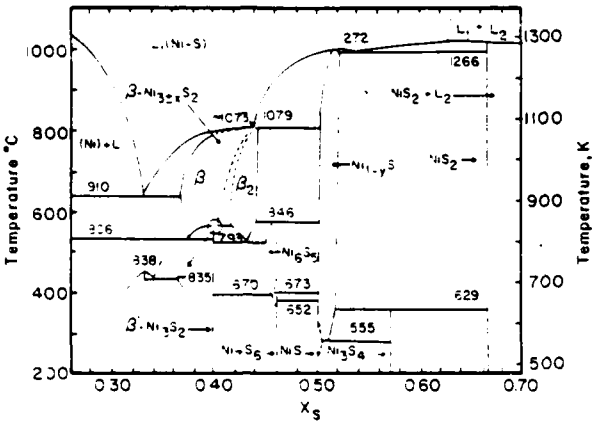

Fig. 1. Phase diagram for the nickel–sulfur system.[4]

al.[4] evaluated literature data in addition to their own and reported a complete phase diagram of the nickel–sulfur system, as shown in Fig. 1. Rau[7] and Lin *et al.*[4] have also determined the sulfur activity in β-$Ni_{3\pm x}S_2$ as a function of sulfur mole fraction and temperature. Based on the sulfur activity-composition data, Rau[7] and Lin *et al.*[4] suggested that high temperature β-$Ni_{3\pm x}S_2$ phase consisted of two different phases, β_1- and β_2-$Ni_{3\pm x}S_2$, in contrast to other investigators.[4–6] However, neither the structure of each phase nor the difference in properties between these two phases has been reported.

Chemical diffusion in β-$Ni_{3\pm x}S_2$ has been reported by Stoklosa and Stringer.[9] No dependence of the chemical diffusion coefficient on composition, x was observed. From density measurements[9] on quenched $Ni_{3\pm x}S_2$ and marker studies after sulfidation of nickel in H_2S/H_2 gas mixtures[10] Stoklosa and Stringer concluded that β-$Ni_{3\pm x}S_2$ is defective in both anion and cation sublattices. They suggested that its chemical formula may be described as $Ni_{3\pm x}S_{2\pm x}$ where $y \simeq 2x$. According to Liné and Hubers[11] on the other hand β-$Ni_{3\pm x}S_2$ has a fcc structure in which nickel atoms are randomly distributed in octahedral and tetrahedral sites of cubic closed-packed framework of sulfur atoms with several nickel vacancies. Based on this structure model, they suggested that the defect structure of β-$Ni_{3\pm x}S_2$ can be described as $Ni_{4-x}\square_xS_2$, where $\square$ is a nickel vacancy. In either model for the defect structure the possibility that β-$Ni_{3\pm x}S_2$ consists of two different phases, β_1- and β_2-$Ni_{3\pm x}S_2$ was not addressed.

In the present study, the activity-composition relations of β-$Ni_{3\pm x}S_2$ were reexamined in order to test the existence of the two phase regions, β_1- and β_2-$Ni_{3\pm x}S_2$. Then, using the relations established in the present study, chemical diffusion coefficients and electrical conductivities of β-$Ni_{3\pm x}S_2$ were measured as functions of composition and temperature.

EXPERIMENTAL

Measurements of Sulfur Activity-Composition Relation

Sulfur activity and composition of β-$Ni_{3\pm x}S_2$ phase were determined by the usual gas equilibration technique between 600 and 750°C. A schematic diagram of the experimental apparatus is shown in Fig. 2. A nickel sheet suspended from a Cahn 1000 microbalance was equilibrated with a gas mixture consisting of H_2S and H_2 at a given temperature. The composition of the phase equilibrated with the gas mixture was determined by continuously weighing the sample. Nickel sheet of 99.999% purity was

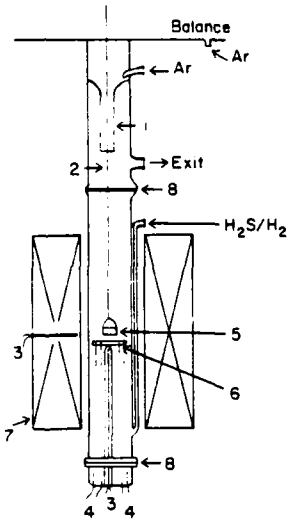

Fig. 2. Reaction chamber for the chemical diffusion and electrical conductivity measurements. (1): gas restriction to protect the balance from H_2S; (2): platinum wire; (3): Pt/Pt–10% Rh thermocouple; (4): platinum lead wires for electrical conductivity measurement; (5): platinum mesh basket, (6): sample for electrical conductivity measurement; (7): furnace, (8): O-ring joint.

supplied by Johnson-Matthey Chemical, Ltd. The nominal impurities (ppm wt.) were Fe = 3, Al, Ca, Cu, Mg, Si, Ag (each) ≤ 1. Nickel samples (20 × 14 × 0.5 mm) were polished on emery paper from 1/0 grit down to 4/0 grit and cleaned with water and trichloroethylene. Before each run, the initial weight of the nickel sample (about 1.13 g) was measured using a Mettler H51AR analytical balance. This weight was used as a standard in calculating the composition of the sample. The nickel sample was suspended from the balance by a platinum wire. The balance was protected from corrosive H_2S by flowing dry Ar gas through the balance chamber and the constriction as shown in Fig. 2. The furnace temperature was controlled within ± 1°C by a P.I.D. temperature controller (Thermac Type D 30, Research Inc.). The temperature of the sample was measured by a Pt/Pt–10% Rh thermocouple positioned just below the sample.

The activity of sulfur a_s in $Ni_{3\pm x}S_2$ phase relative to a standard state of $S_2(g)$ at 1 atm may be obtained from the relationship $a_s = (P_{H_2S}/P_{H_2})(1/K)$. The term K is the equilibrium constant for the reaction, $H_2(g) + \frac{1}{2}S_2(g) = H_2S(g)$ and was computed from the Gibbs free energy of formation of $H_2S(g)$ selected by Mah and Pankratz.[12] The ratio of P_{H_2S}/P_{H_2} is obtained from the flow rate of the gases. Hydrogen sulfide (C.P. grade) supplied by Matheson was dried over two columns of P_2O_5. Hydrogen was passed through a drierite column and a P_2O_5 column to absorb and through heated magnesium chips to remove traces of oxygen and then again through a P_2O_5 column. Argon gas to protect the balance was purified in the same way as hydrogen, except that traces of oxygen impurity in argon gas were removed by heated titanium sponge (800°C). The flow rates of H_2S and H_2 were measured by capillary manometers calibrated by the method of soap bubble displacement. H_2S and H_2 were mixed by passing through a column filled with glass beads. The total flow rate of the gas mixture was 0.81 cm/sec.

Chemical Diffusion Measurements

The chemical diffusion coefficients of $Ni_{3\pm x}S_2$ were measured between 600 and 750°C by the usual gravimetric method[13] using the same experimental apparatus described above. There were difficulties in the preparation of $Ni_{3\pm x}S_2$ sample for the chemical diffusion measurement. Attempts to prepare a flat sample by sulfidizing a nickel sheet into $Nu_{3\pm x}S_2$ in H_2S/H_2 gas mixture failed because the surface of the sample obtained by this method was porous and irregular and large voids were observed at the core. Another attempt to obtain a disk-shaped Ni_3S_2 sample by cutting the Ni_3S_2 rod prepared from a melt of Ni_3S_2 was also not successful. Finally, a relatively compact disk-shaped Ni_3S_2 was obtained by sintering mixtures of NiS and Ni. The NiS (99.99%) and Ni (99.99%) powder were supplied

by Johnson Matthey Chemical, Ltd. Appropriate amounts of NiS and Ni were mixed by mortar and pestle and pressed into a pellet in nickel-plated die. Then, the pellets were sealed in a silica tube under vacuum (10^{-4} Torr) and sintered at 650°C for two months. A typical sample was ~10 mm in diameter ~2 mm in thickness and weighed about 700 mg. Before the run, the exact weight, diameter, and thickness of the sample were measured. The sample was placed in a basket made of platinum mesh which was suspended from the balance by platinum wire.

The measurement of chemical diffusion in $Ni_{3\pm x}S_2$ was carried out as follows. After equilibrating the sample with an H_2S/H_2 gas mixture of a certain composition at constant temperature, the composition of the gas mixture was changed to a new value. The resulting weight change of the sample was recorded as a function of time until the weight of sample became constant. The variation of the weight change with time was analyzed to obtain the chemical diffusion coefficient of $Ni_{3\pm x}S_2$. The details of the analysis will be disussed later. By repeating this procedure, chemical diffusion coefficients of $Ni_{3\pm x}S_2$ were measured as a function of composition of the H_2S/H_2 gas mixture. The composition of the sample equilibrated with the H_2S/H_2 gas mixture of certain composition was calculated using the sulfur activity-composition relations obtained in the present study.

Electrical Conductivity Measurements

A rod-shaped Ni_3S_2 sample for electrical conductivity measurement was prepared from the melt of Ni_3S_2. The dimensions of the sample were approximately 4 mm in diameter and 15 mm in length. The conductivity was measured by the dc four-probe method. Four platinum lead wires were attached to the sample rod, which was placed just below the basket as shown in Fig. 2. The distance between the platinum lead wires is 13 mm for the current measurement and 9 mm for the voltage measurement. Keithley model 225 was used as constant current source and the voltage drop across the sample was measured using a Keithley model 177 voltmeter. Maximum current used in the measurement was ~100 mA, which produced about 100-μV voltage drop across the sample. The conductivity of $Ni_{3\pm x}S_2$ was measured as a function of composition at 650°C. It was assumed that the sample was in equilibrium with the H_2S/H_2 gas mixture at the time of measurement so that the composition of the conductivity sample can be calculated from the sulfur activity-composition relations obtained in the present study.

Also, the electrical conductivity of Ni_3S_2 was measured as a function of temperature between 50° and 750°C. The measurements were carried out under a purified argon gas stream to avoid oxidation of the sample.

RESULTS AND DISCUSSION

Sulfur Activity-Composition Relation

The experimental results obtained in the present study for sulfur activity-composition relation in β-$Ni_{3\pm x}S_2$ are shown in Fig. 3, where the ratios of P_{H_2S} to P_{H_2} in the gas mixtures equilibrated with the sample are shown as a function of mole fraction of sulfur, $X_S = 2/(5 \pm x)$ for the $Ni_{3\pm x}S_2$ phase. There is some departure from linearity in the curves obtained at 600, 650, and 700°C as shown in Fig. 3. This may indicate a β_1- and β_2-$Ni_{3\pm x}S_2$ two phase region.

In order to clarify the two phase regions, the activity-composition data were evaluated in terms of the α function as defined below,

$$\alpha_S = \frac{\ln \gamma_S}{(1 - X_S)^2} \tag{1}$$

where γ_S is the activity coefficient of sulfur and X_S is the mole fraction of sulfur. The activity coefficients were calculated using the activity-composition relations obtained in the present study. The variation of the α function of sulfur with X_S are shown in Fig. 4, where the results by Lin *et al.*[4] are also included. In Fig. 4, the existence of β- and β-$Ni_{3\pm x}S_2$ two phase region at 600, 650, and 700°C can be seen more clearly compared to that in the previous figure. The data at 750°C, however, do not show any evidence of a two phase region. According to Rau[3] and Lin *et al.*,[4] the β_1 and β_2 two-phase region exists up to about 800°C, although the data by Lin *et al.* at 750°C shown in Fig. 4 do not indicate the existence of the two phase region.

Chemical Diffusion Coefficient

If the reequilibration reaction due to a stepwise change in the composition of H_2S/H_2 gas mixture is diffusion-controlled, the variation of weight change due to the reaction with time after an initial period of the reaction is described by the following solution of Fick's second law for diffusion into a finite sample in the form of a thin plate[3]

$$-\ln(1 - \Delta M_t/\Delta M_\infty) = -\ln\frac{8}{\pi^2} + \frac{\tilde{D}\pi^2}{4l^2} \cdot t \tag{2}$$

where $\tilde{D}$ is the chemical diffusion coefficient, l is a half of the sample thickness, and ΔM_t and ΔM_∞ are weight change at time, t, and total weight change after reequilibration, respectively. Equation (2) implies that a plot of $-\ln(1-\Delta M_t/\Delta M_\infty)$ against t fall on a straight line and the slope of the line gives the chemical diffusion coefficient, $\tilde{D}$.

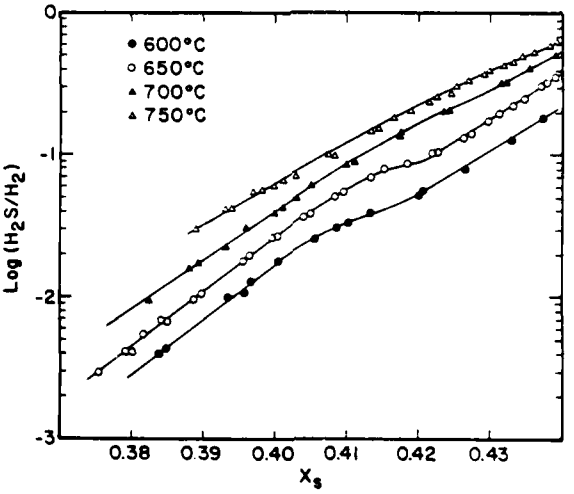

Fig. 3. Activity of sulfur in H_2S/H_2 ratio as a function of sulfur mole fraction for β-$Ni_{3+x}S_2$.

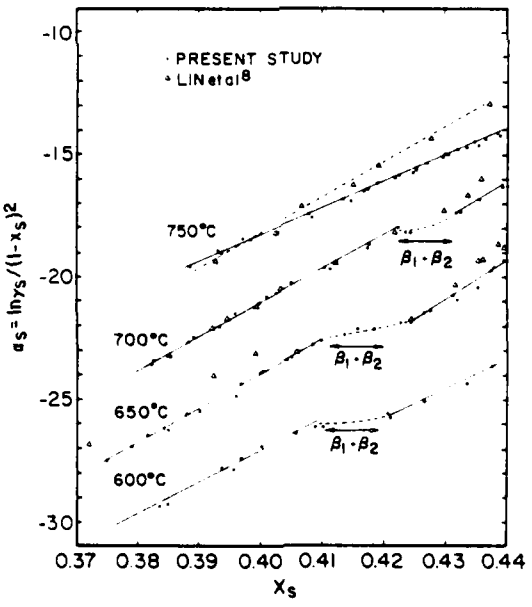

Fig. 4. The α function of sulfur as a function of sulfur mole fraction for β-$Ni_{3+x}S_2$.

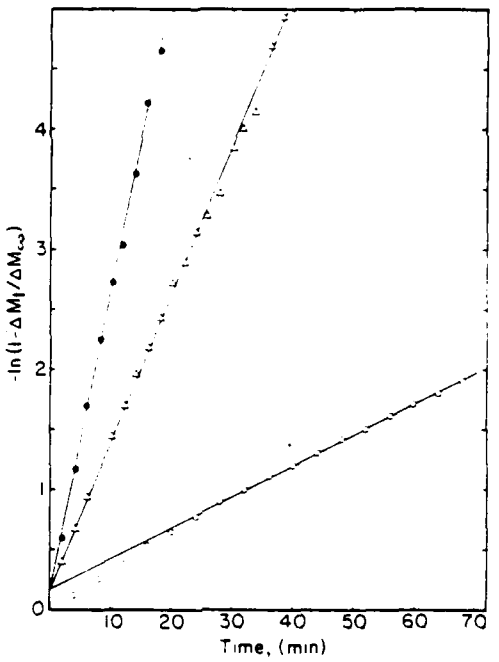

Fig. 5. Plots of $-\ln(1-\Delta M_t/\Delta M_\infty)$ vs. t. ●: P_{H_2S}/P_{H_2} = 0.102 to 0.084 at 650°C. ○: P_{H_2S}, P_{H_2} = 0.045 to 0.060 at 700°C. △: P_{H_2S}, P_{H_2} = 0.029 to 0.041 at 750°C.

The use of Eq. (2) to determine $\tilde{D}$ may not be completely applicable for the geometry of the sample used in the present study because the diffusion through the radical direction of the sample may not be negligible. In spite of this limitation, we estimated the chemical diffusion coefficient by using Eq. (2) for the sake of simplicity. Figure 5 shows the typical plots of $-\ln(1-\Delta M_t/\Delta M_\infty)$ vs. t. The plots are linear and the intercept of the ordinate is about 0.2, which is close to $-\ln 8/\pi^2$, expected by Eq. (2). A typical value of ΔM_∞ was about 6 mg when total weight of the sample was about 700 mg. These facts may indicate that the reequilibration reaction is controlled by diffusion and the effect of radial diffusion is minimum. Although Stoklosa and Stringer[9] have reported that the diffusion-controlled reactions were observed only when the measurements were carried out in the H_2S/H_2 gas mixtures containing 10% H_2S, we found the similar linear plots in the gas mixtures of all the composition studied when the tem-

perature was above 650°C. The present study at 600°C showed that the reaction followed linear kinetics in the initial period of the reaction. Therefore, no chemical diffusion coefficient was determined at 600°C in the present study.

The chemical diffusion coefficients of β-$Ni_{3\pm x}S_2$ obtained in the present study are shown as a function of mole fraction of sulfur, X_s, in Fig. 6 for 600°C and 700°C and in Fig. 7 for 750°C. The composition of the sample corresponding to a certain determined chemical diffusion coefficient was considered to be a mean between initial and final composition. A typical composition change was ~0.005 in mole fraction of sulfur, X_s. In Fig. 6 the composition range for the β_1- and β_2-$Ni_{3\pm x}S_2$ two phase region is also indicated for both temperatures. As seen in Figs. 6 and 7, the chemical diffusion coefficients of β_1-$Ni_{3\pm x}S_2$ increase with increase in X_s, reach a maximum at the stoichiometric compositions $X_s = 0.4$ and then decrease with further increase in X_s. In the β_2-$Ni_{3\pm x}S_2$ region, the chemical diffusion coefficient seems to increase with increase in X_s. The chemical diffusion coefficient at 750°C shown in Fig. 7 decreases continuously with X_s ($X_s \geq 0.4$) and does not show any evidence for the existence of β_2-$Ni_{3\pm x}S_2$. This agrees with the absence of a β_1- and β_2-$Ni_{3\pm x}S_2$ two-phase region in α function at 750°C (Fig. 4).

According to Wagner's theory[13-15] of chemical diffusion in a binary-compound semiconductor, the chemical diffusion coefficient should be essentially independent of composition for systems exhibiting small devi-

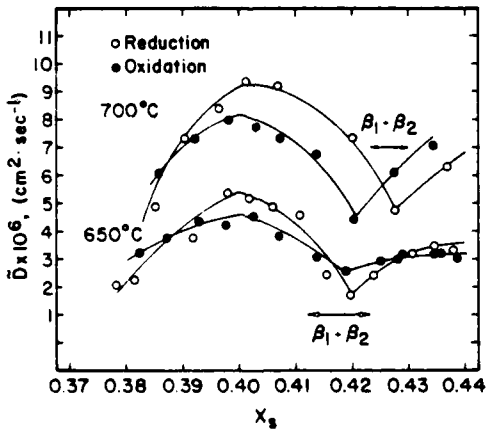

Fig. 6. Chemical diffusion coefficient, $\tilde{D}$ as a function of sulfur mole fraction for β-$Ni_{3\pm x}S_2$ at 650° and 700°C.

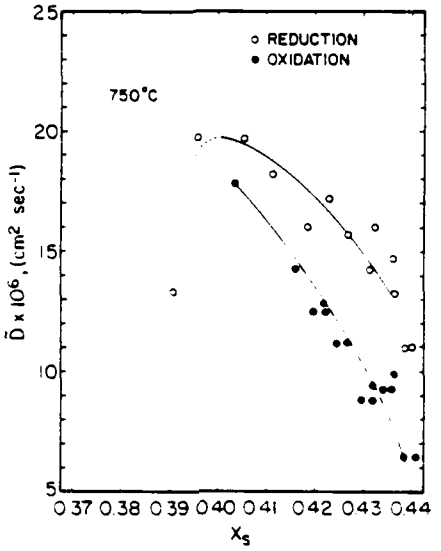

Fig. 7. Chemical diffusion coefficient, $\tilde{D}$ as a function of sulfur mole fraction for β-$Ni_{1+x}S_2$ at 750°C.

ations from stoichiometry. Deviations from this behavior have been found in many compounds with significant nonstoichiometry such as FeO,[16,17] MnO[17] Cu_2S,[18] and Cr_2N[19] In the case of FeO and MnO the chemical diffusion coefficient decreases with the concentration of the majority lattice defect, the increase in cation vacancies, while the tracer diffusion coefficient, and of course, the self-diffusion coefficient increase with increasing defect concentration, as expected. For Cr_2N, the chemical diffusion coefficient shows a minimum of $y = 0.85 \sim 0.9$ in Cr_2N_y between 1050 and 1200°C.[19,20] The decrease in the chemical diffusion coefficient with increasing defect concentration is generally considered to be due to increasing energetic interactions between various defects, such as cation vacancies and electron holes and/or vacancy-vacancy interactions.[13] So far, there has been no theoretical model which can explain the defect concentration dependence of the chemical diffusion coefficient for compounds having large deviations from stoichiometry. Accordingly, it is not possible to explain the compositional dependence of the chemical diffusion coefficient for β_1- and β_2-$Ni_{1+x}S_2$ observed in the present study, since the defect structure of β-$Ni_{1+x}S_2$ has not yet been established as discussed in the

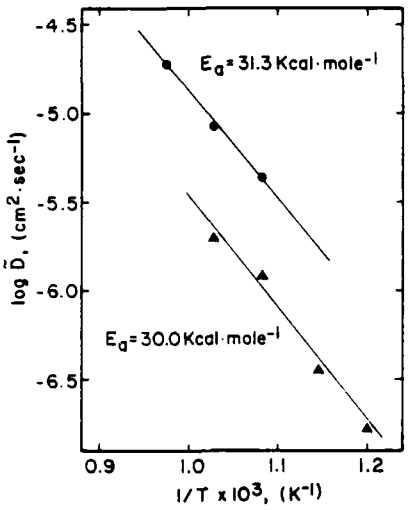

Fig. 8. Temperature dependence of the chemical diffusion coefficient, $\tilde{D}$ for β_1-$Ni_{3\pm x}S_2$. ●: Present study ($X_s = 0.400$); ▲: Stoklosa and Stringer.[9]

previous section. The presence of a maximum at the stoichiometric composition, $X_s = 0.4$ in the chemical diffusion coefficients of β_1-$Ni_{3\pm x}S_2$ may, however, indicate that the defect structure of hypostoichiometric $Ni_{3-x}S_2$ is different from that for hyper stoichiometric $Ni_{3-x}S_2$.

As seen in Figs. 6 and 7, the chemical diffusion coefficients for reduction of β_1-$Ni_{3\pm x}S_2$ are ~10–40% higher than those for oxidation. These dissimilar kinetics for reduction and oxidation in reequilibration of oxides have also been found in FeO[13,21] MnO[13,22] and NiO–Cr_2O_3[23,24] solid solutions. These observations indicate that surface processes are at least partially rate-determining in the reequilibration reaction.

The temperature dependence of the chemical diffusion coefficients in β_1-$Ni_{3\pm x}S_2$ is shown for only one composition, $X_s = 0.40$ in Fig. 9, where the results by Stoklosa and Stringer[9] are also included. The present data in Fig. 9 are the mean of the values obtained in oxidation and in reduction. The data by Stoklosa and Stringer were obtained from the reequilibration reaction in which the composition of the H_2S/H_2 gas mixture was changed from 2% H_2S to 10% H_2S at each temperature. Therefore, the composition of their samples may be different at different temperatures. The activation energy obtained in the present study was $E_a = 31.3$ kcal·mole^{-1}, which is

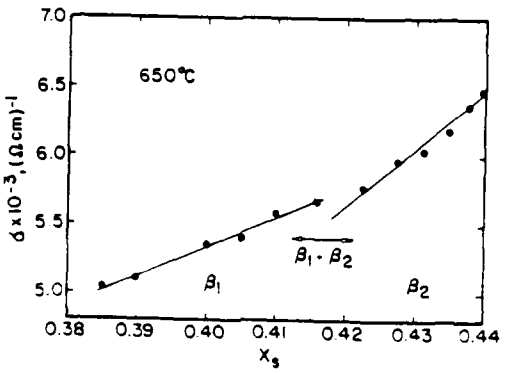

Fig. 9. Electrical conductivity as a function of sulfur mole fraction for β-$Ni_{1+x}S_2$ at 650°C.

in agreement with E_a = 30 kcal · mole^{-1} reported by Stoklosa and Stringer.[9] The discrepancies in the values of the chemical diffusion coefficients between these two sets of experiments are probably due to the difference in both the sample preparations, especially the sample geometry, and the composition of the samples for which the chemical diffusion coefficients were obtained.

Electrical Conductivity

The compositional dependence of electrical conductivities of β-$Ni_{1+x}S_2$ obtained in the present study at 650°C are shown in Fig. 9. The conductivity is very high and increases with increasing mole fraction of sulfur, X_s, which is in accord with the results by Brusq *et al.*[25] A sudden change in the slope of conductivity-composition relation as shown in Fig. 9 may be further evidence for the existence of the β_1- and β_2-$Ni_{1+x}S_2$ two-phase region. It should be noted that a chemical diffusion study in β-$Ni_{1+x}S_2$ by electrical conductivity measurements as has been done for CoO[26] and NiO[26,27] would be less fruitful because the change in electrical conductivity with composition is so small.

The variation of the electrical resistivity of Ni_3S_2 with temperature is shown in Fig. 10. The resistivity increases linearly with temperature. The sudden change in the resistivity at 550°C may correspond to the phase transition of low temperature β'-Ni_3S_2 to high temperature β_1-$Ni_{1+x}S_2$ observed in phase equilibrium studies by other investigators.[4,5] As seen in Fig. 10, the temperature dependence of electrical resistivity for β_1-$Ni_{1+x}S_2$ seems to be even lower than that for β'-Ni_3S_2.

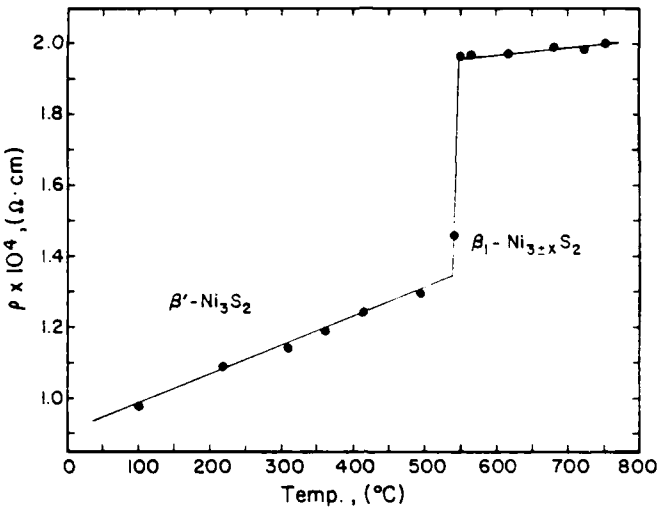

Fig. 10. Electrical resistivity as a function of temperature for Ni_3S_2.

ACKNOWLEDGEMENT

This research was supported by the Army Research Office under contracts DAAG 29-80-C-0049 and DAAG 29-81-K-0109.

REFERENCES

1. H. Nakai and H. Takazawa, *Nippon Kinzoku Grakkai-shi*, **40**, 466 (1976).
2. C. S. Giggins and F. S. Pettit, *Oxid. Met.* **14**, 363 (1980).
3. K. L. Luthra and W. L. Worrell, *Met. Trans.* **9A**, 1055 (1978).
4. T. Rosenqvist, *J. Iron Steel Inst.* **176**, 37 (1954).
5. G. Kellerud and R. A. Yund, *J. Petrology*, **3**, 126 (1962).
6. G. Line and M. Laffitte, *Comptes Rendus Hebdomaires des Séances de l'Academie des Sciences (Paris)*, **256**, 3306 (1963).
7. H. Rau, *J. Phys. Chem. Solids*, **37**, 929 (1976).
8. R. Y. Lin, D. C. Hu, and Y. A. Chang, *Met. Trans.* **9B**, 531 (1978).
9. A. Stoklosa and J. Stringer, *Oxid. Met.* **11**, 277 (1977).
10. A. Stoklosa and J. Stringer, *Oxid. Met.* **11**, 263 (1977).
11. G. Line and M. Huber, *Comptes Rendus Hebdomaires des Séances de l'Académie des Sciences (Paris)*, **256**, 3118 (1963).
12. A. D. Mah and I. B. Pankratz, Bureau of Mines Bulletin 668, Washington, D.C., (U.S. Government Printing Office 1976).
13. P. E. Childs, L. W. Laub, and J. B. Wagner, Jr. *Proc. Br. Ceram. Soc.* **19**, 29 (1971).
14. C. Wagner, *Z. Physik. Chem.* **B11**, 139 (1930).
15. C. Wagner, *Z. Physik. Chem.* **B32**, 447 (1936).

16. R. L. Levin and J. B. Wagner, Jr., *Trans. Metall. Soc. AIME*, **233**, 159 (1965).
17. P. E. Childs and J. B. Wagner, Jr., Proceedings of the International Conference "Heterogeneous Kinetics at Elevated Temperatures" Philadelphia, 1969, G. R. Belton and W. L. Worrell eds., (New York, Plenum Press, 1970).
18. K. Weiss, *Ber. Bunsenges. Physik. Chem.* **73**, 338 (1969).
19. T. Mills, *Oxid. Met.* **15**, 447 (1981).
20. T. Mills, *Oxid. Met.* **15**, 437 (1981).
21. J. Darèn, J. Nowotny, and M. Rekas, *Rocz. Chem.* **46**, 1495 (1972).
22. J. B. Price, Ph.D. thesis, Northwestern University (August 1968).
23. J. Nowotny, J. Obłakowski, A. Sadowski, and J. B. Wagner, Jr., *Oxid. Met.* **14**, 437 (1980).
24. J. Nowotny and J. B. Wagner, Jr., *Oxid. Met.* **169**, 15 (1981).
25. H. L. Brusq, J. P. Delmaike, and F. Marion, *C.R. Acad. Sci. Paris*, **273**, 139 (1971).
26. J. B. Price and J. B. Wagner, Jr., *Z Physik. Chem. N. F.* **49**, 257 (1966).
27. R. Morlotti, *Z. Naturforsch.* **24A**, 441 (1969).

Extended Abstract No. 11, The Electrochemical Society , Cincinnati, OH May 6-11, 1984.

DIFFUSION OF SULFUR IN $Ni_{3\pm x}S_2$

G.M. Mehrotra, V.B. Tare and J.B. Wagner, Jr.
Center for Solid State Science
and Departments of Chemistry,
Mechanical and Aerospace Engineering
and Physics
Arizona State University, Tempe, AZ 85287

$Ni_{3\pm x}S_2$ is often present as one of the corrosion products of nickel in sulfur-containing atmosphere. It has been postulated[1] that, under certain conditions, the corrosion product consists of a continuous network of Ni_3S_2 and that the corrosion rates are governed by the diffusion through the interconnecting nickel sulfide. The knowledge of the rates of transport of nickel and sulfur in $Ni_{3\pm x}S_2$ is therefore important to the understanding of the mechanism of corrosion of nickel. Chemical diffusion in $Ni_{3\pm x}S_2$ has been studied by Yagi and Wagner[2]. However, the contribution of sulfur to the chemical diffusivity is not known. This paper presents the results of our measurements of diffusivity of sulfur-35 in $Ni_{3\pm x}S_2$.

Two compositions of $Ni_{3\pm x}S_2$ containing 40 and 42 atom percent sulfur were prepared by heating, in an evacuated quartz tube, mixtures of ouratronic grade (99.999% pure) nickel powder and 99.99% pure sulfur or 99.99% pure NiS, initially at ~700°C for 2-3 days and subsequently at 800°C for one day. Some of the compounds were melted in evacuated quartz tubes of ~8mm I.D. and subsequently quenched so as to obtain rods of $Ni_{3\pm x}S_2$. Pellets, ~3-4mm in height, were then cut from these rods. These pellets were of >95% theoretical density. The prepared $Ni_{3\pm x}S_2$ compounds were characterized by hydrogen reduction to determine Ni/S ratio and by X-ray diffraction for phase identification. For a diffusion anneal, a pellet of $Ni_{3\pm x}S_2$, together with some sulfur-35 in a quartz boat, was sealed in a quartz tube without evacuation. The sealed capsule was then annealed at a desired temperature (695-775°C) and for a desired duration (2-20 hrs.). The penetration profiles of sulfur were obtained by successive grinding and measuring the residual activity of sulfur using a Nuclear Chicago (model 1152) counter.

The diffusivity of sulfur in $Ni_{3\pm x}S_2$ at 695°C and 775°C has been estimated to be of the order of $\sim 10^{-10}$ and 10^{-8} cm^2/sec, respectively. These values of diffusivity are much smaller than the chemical diffusivity[2] of $Ni_{3\pm x}S_2$ ($\sim 8 \times 10^{-6}$ cm^2/sec for stoichiometric Ni_3S_2 and $\sim 5 \times 10^{-6}$ cm^2/sec for $Ni_{3-x}S_2$ containing 42 atom % sulfur at 700°C). This indicates that the contribution of sulfur diffusion to the chemical diffusivity is extremely small. Further, our measurements with the two compositions (40 and 42 atom % sulfur) show that there is no significant difference in the rates of diffusion of sulfur in $Ni_{3\pm x}S_2$ of different compositions. This would suggest that, if the diffusion of sulfur is assumed to be due to the presence of defects in sulfur sub-lattice in Ni_3S_2, the change in the Ni/S ratio does not alter this defect concentration and that the defect structure and hence the deviation from stoichiometry in Ni_3S_2 is presumably due to the changes in the concentration of nickel in a relatively stable framework of sulfur sublattice.

Acknowledgement

This research was supported by the Army Research Office under contract DAAG-29-81-K 0109 and a grant through the Center for Solid State Science.

References

1. K. L. Luthra and W. L. Worrell, Met. Trans, 9A (1978) 1055.

2. H. Yagi and J. B. Wagner, Jr., Oxidation of Metals, 18, Nos. 1/2 (1982) 41.

END

FILMED

10-85

DTIC